Isospin dependent nucleon-nucleus optical potential with Skyrme interactions

Qing-biao Shen (申庆彪), Yin-lu Han (韩银录), and Hai-rui Guo (郭海瑞)
China Institute of Atomic Energy, P. O. Box 275(41), Beijing 102413, People's Republic of China
(Received 6 May 2009; published 18 August 2009)

In this paper, the isospin dependent nucleon-nucleus optical potential theory is introduced on the basis of the effective Skyrme interactions. From the view of the many-body theory, the nucleon optical potential can be identified with the mass operator of the one-particle Green function. The first and second order mass operators of the one particle Green function in nuclear matter are derived, and the real and imaginary parts of the optical potential for finite nuclei are obtained as usual by applying a local density approximation. Our results, in most cases, can be derived and expressed analytically. From an extensive comparison with experimental data of various quantities of interests, it is concluded that for certain versions of Skyrme interactions without parameter adjusting the agreement between theory and experiments can be obtained satisfactorily. We define the ratio of the difference and summation of the neutron and proton nonelastic cross sections as the isospin effect value. The calculated results show that the isopin effect value decreases as the incident energy increases and increases as the asymmetric parameter $\alpha_0 = (N\text{-}Z)/A$ of the target nucleus increases.

DOI: 10.1103/PhysRevC.80.024604 PACS number(s): 24.10.Ht, 21.30.Fe, 24.10.Cn, 25.40.−h

I. INTRODUCTION

The optical model is one of the most fundamental theoretical tools in the analysis of nuclear reaction data. The phenomenological optical potential with many adjustable parameters can reproduce the experimental data quite well, but cannot predict the unknown data with certainty. Thus, the derivation of the optical potential from the more basic theory is one of the most important problems in nuclear theory, which is of both theoretical and practical interest.

As early as 1959, Bell and Squires [1,2] show that from the view of the many-body theory the nucleon optical potential can be identified with the mass operator of the one-particle Green function. This identification makes it possible to utilize the many-body theory technique to obtain a microscopic optical potential (MOP) without free parameters. More specifically, two different approaches have been formulated. One is the "nuclear matter approach" [3–5] in which one starts from the realistic nuclear force to calculate the mass operator via the Brueckner-Hartree-Fock (BHF) approximation in nuclear matter. From here the MOP for finite nuclei is obtained by making a local density approximation (LDA). Thus, the MOP for all target nuclei can be obtained in principle. The other approach is the "nuclear structure approach" [6,7], in which one only applies the two-body effective nuclear force via the Hartree-Fock (HF) method, in conjunction with the random phase approximation (RPA), to calculate the MOP for some specific finite nuclei. Thus, the second approach involves specific features of the nuclear structure of the target nucleus, while the "nuclear matter approach" involves the effects of the nuclear structure only in an average way (via the LDA).

Both approaches have their merits and limitations. Since we are more interested in the global properties of the optical potential, encouraged by the success of the nuclear matter approach and the phenomenological Skyrme interactions, we adopt a simpler and more economical way for MOP calculation [8–14]. We calculate the mass operator of the one-particle Green function only up to the second order in nuclear matter by using the Skyrme interactions. The optical potential for the finite nuclei is then obtained as usual by LDA. Since the Skyrme interactions can be viewed as effective G matrices in the Hartree-Fock calculations [15,16], we let only the first-order mass operator $M(1)$ represent the real part of the optical potential and consider the imaginary part of the second-order mass operator $M(2)$ as the imaginary part of the optical potential. The spin-orbit potential has also been obtained approximately. While this approach is not as basic as the MOP based on the realistic nuclear force, by using the Skyrme interaction we can get very simple, in most cases analytical, expressions for the optical potential, which is physically more transparent and easier to apply. In addition, at present there exist many sets of Skyrme interactions, most of which are quite successful in the calculations of the average ground state properties of nuclei. As is known, the different Skyrme interactions give the same good agreement for HF calculations but yield quite different results for excited states [17]. Thus, from another point of view our work might provide a good testing ground for different Skyrme interactions in reproducing not only the nuclear ground state properties but also the excited state properties of nucleus.

Moreover, much efforts [18–20] has been devoted to studying the (off-shell) energy-dependent single-particle potential [off-shell mass operator $M(k,E)$ where E can differ from the on-shell energy]. However, most of these studies are based on the effective interactions which seem too simple and not very realistic. On the other hand, the standard Brueckner-Hartree-Fock approximation is very hard to carry out with enough numerical accuracy and clear physical interpretation. In addition, it only sums particle-particle ladders without the so-called correlation term. Thus, it seems very desirable that one could use a rather realistic effective nucleon-nucleon interaction as a basis for deriving a single-particle potential which is both complex and dynamic in an unified and consistent way. Extending our studies to (off-shell) energy-dependence of the single-particle potential [21–23], we calculate the off-shell imaginary part $W(k,E)$ of the second-order mass operator $M(2)$ in nuclear matter analytically with those Skyrme interactions which give

TABLE I. The parameters of the conventional Skyrme force.

	t_0 MeV · fm^3	t_1 MeV · fm^5	t_2 MeV · fm^5	t_{03} MeV · fm^6	x_0	W_0 MeV · fm^5
SII	−1169.9	585.6	−27.1	9331.1	0.34	105
SIII	−1128.75	395.0	−95.0	14000	0.45	120
SIV	−1205.6	765.0	35.0	5000	0.05	150
SV	−1248.29	970.56	107.22	0	−0.17	150
SVI	−1101.81	271.67	−138.33	17000	0.583	115

"good" optical potential. The real part of $M(2)$ is then obtained with the help of the dispersion relation. From here the effective mass, the single-particle widths, the spectral function and the hole occupation numbers are calculated and subsequently compared with available empirical values such that reasonable agreement is obtained. We also extend our theoretical method to calculate the temperature-dependent nucleon microscopic optical potential [24–26] in which some interesting results are uncovered.

In recent years, new experimental data (especially above 20 MeV) have been produced, that can be used to examine our theoretical method. Having performed calculations and comparisons with nearly every available Skyrme interactions, our results show that there indeed exist some sets of Skyrme interactions with which we can obtain MOP in agreement with the experimental data. Moreover, the MOP we obtain is isospin dependent. The nuclear reaction isospin effect includes the difference of the reaction cross sections induced by neutron and proton as well as the effect of the rich neutron degree of the target nucleus. We define the ratio of the difference and summation of the neutron and proton nonelastic cross sections as the isospin effect value which is studied. The formulas of the MOP on the basis of the effective Skyrme interactions are also reviewed in this paper.

In Sec. II, the basic theory and formulas are introduced. In Sec. III, the formulation of the nucleon microscopic optical potential is presented. The calculated results and analysis are given in Sec. IV. Finally, a summary is given in Sec. V.

II. BASIC THEORY AND FORMULAS

A. Skyrme interactions

At present there exist many sets of Skyrme interactions. They can be summarized as follows.

1. The conventional Skyrme force

The two-body interactions of the conventional Skyrme force are as follows [15]:

$$V_{12}(\vec{r}) = t_0(1+x_0P^\sigma)\delta(\vec{r}) + \tfrac{1}{2}t_1(\vec{k}'^2\delta(\vec{r}) + \delta(\vec{r})\,\vec{k}^2) + t_2\vec{k}'\cdot\delta(\vec{r})\vec{k} + iW_0(\vec{\sigma}_1+\vec{\sigma}_2)\cdot\vec{k}'\times\delta(\vec{r})\vec{k}, \quad (2.1)$$

where

$$\vec{r} = \vec{r}_1 - \vec{r}_2, \quad (2.2)$$

$$\vec{k} = \frac{1}{2i}\left(\vec{\nabla}_1 - \vec{\nabla}_2\right), \quad \text{acting on the right,}$$
$$\vec{k}' = -\frac{1}{2i}\left(\vec{\nabla}_1 - \vec{\nabla}_2\right), \quad \text{acting on the left.} \quad (2.3)$$

P^σ is the spin exchange operator and $\vec{\sigma}$ is the Pauli spin matrx. The three-body interaction has the following form:

$$W_{123}(\vec{r}_1,\vec{r}_2,\vec{r}_3) = t_{03}\delta(\vec{r}_1-\vec{r}_2)\delta(\vec{r}_2-\vec{r}_3). \quad (2.4)$$

In Eqs. (2.1) and (2.4) t_0, t_1, t_2, t_{03}, x_0, and W_0 are the parameters of the Skyrme interaction. The conventional Skyrme interaction parameters SII [15] and SIII∼SVI [27] are listed in Table I.

2. The extended Skyrme force

The extended Skyrme force is only a two-body effective interaction described by a density- and momentum-dependent delta function. It can be written in a unified form as follows:

$$\begin{aligned} V_{12}(\vec{R},\vec{r}) &= t_0(1+x_0P^\sigma)\delta(\vec{r}) + \tfrac{1}{6}t_3(1+x_3P^\sigma)\rho^a(\vec{R})\delta(\vec{r}) \\ &+ \tfrac{1}{2}t_1(1+x_1P^\sigma)\,(\vec{k}'^2\delta(\vec{r}) + \delta(\vec{r})\,\vec{k}^2) \\ &+ \tfrac{1}{2}t_4(1+x_4P^\sigma)\,(\vec{k}'^2\rho(\vec{R})\delta(\vec{r}) + \delta(\vec{r})\rho(\vec{R})\,\vec{k}^2) \\ &+ t_2(1+x_2P^\sigma)\vec{k}'\cdot\delta(\vec{r})\vec{k} + t_5(1+x_5P^\sigma)\vec{k}' \\ &\cdot\rho(\vec{R})\delta(\vec{r})\vec{k} + iW_0(\vec{\sigma}_1+\vec{\sigma}_2)\cdot\vec{k}'\times\delta(\vec{r})\vec{k}, \end{aligned} \quad (2.5)$$

where

$$\vec{R} = \tfrac{1}{2}(\vec{r}_1+\vec{r}_2). \quad (2.6)$$

From Skyrme-Hartree-Fock theory [15] we can see that the three-body interaction given by Eq. (2.4) is equivalent to a two-body density-dependent interaction

$$V_{12} = \tfrac{1}{6}t_{03}(1+P^\sigma)\rho(\vec{R})\delta(\vec{r}). \quad (2.7)$$

The extended Skyrme interaction parameters GS1∼GS6 [17], SG0I and SG0II [28], Ska and Skb [29], SKM [30], SGI, and SGII [31], and SkMP [32] are listed in Table II.

TABLE II. The parameters of the extended Skyrme force.[a]

	t_0 MeV $\cdot$ fm^3	t_1 MeV $\cdot$ fm^5	t_2 MeV $\cdot$ fm^5	t_3	t_4 MeV $\cdot$ fm^8	x_0	x_1	x_2	x_3	x_4	W_0 MeV $\cdot$ fm^5	α
GS1	−1268	887	−77.3	14485	−1853	0.15	0	0	1	1	105	1
GS2	−1177	670	−49.7	11054	−775	0.124	0	0	1	1	105	1
GS3	−1037	336	−7.3	5774	883	0.074	0	0	1	1	105	1
GS4	−1242	760	−146.2	19362	−2157	0.206	0	0	1	1	105	1
GS5	−1152	543	−118.6	15989	−1079	0.182	0	0	1	1	105	1
GS6	−1012	209	−76.3	10619	579	0.139	0	0	1	1	105	1
SGOI	−1089	558.8	−83.7	8272	0	0.412	0	0	0	0	130	1
SGOII	−2248	558.8	−83.7	11224	0	0.715	0	0	0	0	130	1/6
Ska	−1602.78	570.88	−67.70	8000	0	−0.02	0	0	−0.286	0	125	1/3
Skb	−1602.78	570.88	−67.70	8000	0	−0.165	0	0	−0.286	0	125	1/3
SKM	−2645	385	−120	15595	0	0.09	0	0	0	0	130	1/6
SGI	−1603	515.9	84.5	8000	0	−0.02	−0.5	−1.731	0.1381	0	115	1/3
SGII	−2645	340	−41.9	15595	0	0.09	−0.0588	1.425	0.06044	0	105	1/6
SkMP	−2372.24	503.623	57.2783	12585.3	0	−0.157563	−0.402886	−2.95571	−0.267933	0	160	1/6

[a] $t_5(\text{MeV}\cdot\text{fm}^8) = 0$, $x_5 = 0$.

B. Mass operator

The Hamiltonian simultaneously composed of the two-body and three-body interactions can be written as

$$H = H_0 + H_1, \tag{2.8}$$

where

$$H_0 = \sum_i (t_i + U_i), \tag{2.9}$$

$$H_1 = \frac{1}{2!}\sum_{i\neq j} V_{ij} + \frac{1}{3!}\sum_{i\neq j\neq k} W_{ijk} - \sum_i U_i. \tag{2.10}$$

Here H_o is the single-particle Hamiltonian, H_1 is the residual interaction, and U_i is the mean field of the single-particle.

Let the single-particle Green function be written as $G_{\alpha\beta}(t_1 - t_2)$ and expand it into the perturbation series. The Fourier transformation for the one-particle Green function is defined as

$$G_{\alpha\beta}(\omega) = \int_{-\infty}^{\infty} \mathrm{d}t\, e^{\frac{i}{\hbar}\omega t} G_{\alpha\beta}(t). \tag{2.11}$$

Next, applying the Fourier transformation to $G_{\alpha\beta}(t_1 - t_2)$ based on Eq. (2.11), we obtain

$$G_{\alpha\beta}(\omega) = \delta_{\alpha\beta} G^{(0)}_{\alpha}(\omega) + G^{(1)}_{\alpha\beta}(\omega) + G^{(2)}_{\alpha\beta}(\omega) + \cdots \tag{2.12}$$

which satisfies the Dyson equation

$$G_{\alpha\beta}(\omega) = \delta_{\alpha\beta} G^{(0)}_{\alpha}(\omega) + G^{(0)}_{\alpha\beta}(\omega) \times \sum_{\gamma} [U_{\alpha\gamma} - M_{\alpha\gamma}(\omega)] G_{\gamma\beta}(\omega), \tag{2.13}$$

where $U_{\alpha\gamma}$ is the mean field, $M_{\alpha\gamma}(\omega)$ is the mass operator, and

$$M_{\alpha\gamma}(\omega) = M^{(1)}_{\alpha\gamma}(\omega) + M^{(2)}_{\alpha\gamma}(\omega) + \cdots \tag{2.14}$$

The mass operator $M_{\alpha\alpha}(E)$ can be identified with the optical model potential for the scattering process with the energy of E.

Figure 1 shows the first order Feynman diagrams of the one-particle Green functions. The dashed line in Fig. 1(a) represents the mean field. Figures 1(b) and 1(c) correspond to the contributions by two-body and tree-body interactions, respectively. Now, the HF mean field $U_{\alpha\alpha}$ is expressed as

$$U_{\alpha\alpha} = M^{(1)}_{\alpha\alpha} = \sum_{\rho} V_{\alpha\rho,\alpha\rho} n_\rho + \frac{1}{2}\sum_{\rho\delta} W_{\alpha\rho\delta,\alpha\rho\delta} n_\rho n_\delta, \tag{2.15}$$

where

$$n_\rho = \begin{cases} 1, & \text{below the Fermi surface} \\ 0, & \text{above the Fermi surface} \end{cases}. \tag{2.16}$$

On the right-hand side of Eq. (2.15) the first term comes from the contribution of the two-body interactions and the second term is that of the three-body interactions. Their matrix elements are, respectively,

$$V_{\alpha\rho,\alpha\rho} = \langle \alpha\rho | V | \alpha\rho \rangle_A, \tag{2.17}$$

$$W_{\alpha\rho\delta,\alpha\rho\delta} = \langle \alpha\rho\delta | W | \alpha\rho\delta \rangle_A, \tag{2.18}$$

where A denotes the antisymmetrization.

The 15 second order Feynman diagrams of the one-particle Green functions in Fig. 2 can be offset with the mean field chosen by Eq. (2.15). The second order mass operator obtained by seven second order Feynman diagrams in Fig. 3 are as

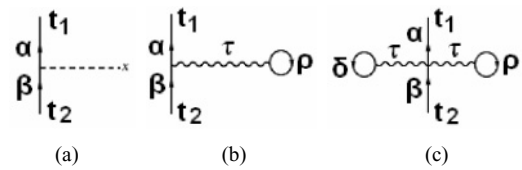

FIG. 1. First order Feynman diagrams of the one-particle Green functions.

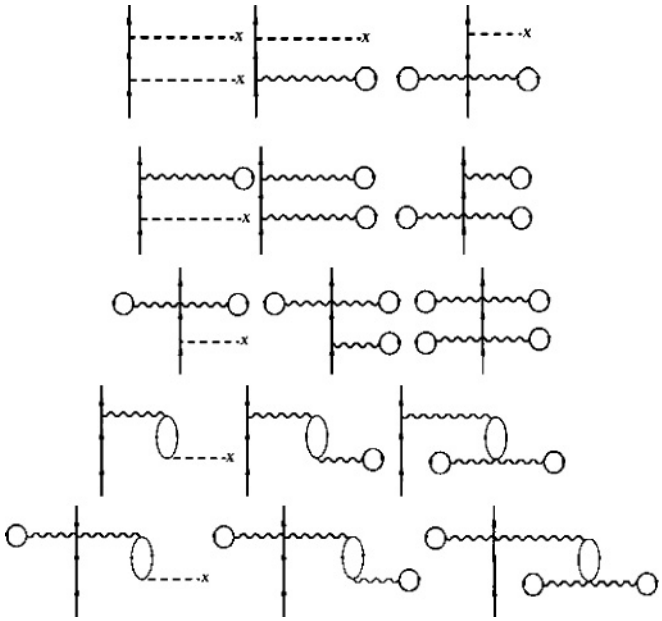

FIG. 2. Second order Feynman diagrams of the one-particle Green functions which can be offset by the mean field.

follows:

$$M^{(2)}_{\alpha\alpha}(\omega) = \sum_{\lambda\mu v} \frac{(1-n_\lambda)(1-n_\mu)n_v}{\omega+\varepsilon_v-\varepsilon_\lambda-\varepsilon_\mu+i\varepsilon} A_{\alpha\lambda\mu v\alpha} + \sum_{\lambda\mu v\xi\zeta} \frac{(1-n_\lambda)(1-n_\mu)(1-n_\xi)n_v n_\zeta}{\omega+\varepsilon_v+\varepsilon_\zeta-\varepsilon_\lambda-\varepsilon_\mu-\varepsilon_\xi+i\varepsilon} B_{\alpha\lambda\mu v\xi\zeta\alpha} + \sum_{\mu v\xi\zeta} \frac{(1-n_\mu)(1-n_\xi)n_v n_\zeta}{\varepsilon_v+\varepsilon_\zeta-\varepsilon_\mu-\varepsilon_\xi+i\varepsilon} C_{\alpha\mu v\xi\zeta\alpha}, \quad (2.19)$$

where

$$A_{\alpha\lambda\mu v\alpha} = \frac{1}{2}V_{\alpha v,\lambda\mu}V_{\lambda\mu,\alpha v} + \frac{1}{2}\left[V_{\alpha v,\lambda\mu}\left(\sum_\rho W_{\lambda\mu\rho,\alpha v\rho}n_\rho\right) + \left(\sum_\rho W_{\alpha v\rho,\lambda\mu\rho}n_\rho\right)V_{\lambda\mu,\alpha v}\right] + \frac{1}{2}\left(\sum_\rho W_{\alpha v\rho,\lambda\mu\rho}n_\rho\right)\left(\sum_\delta W_{\lambda\mu\delta,\alpha v\delta}n_\delta\right), \quad (2.20)$$

$$B_{\alpha\lambda\mu v\xi\zeta\alpha} = \frac{1}{12}W_{\alpha v\zeta,\lambda\mu\xi}W_{\lambda\mu\xi,\alpha v\zeta}, \quad (2.21)$$

$$C_{\alpha\mu v\xi\zeta\alpha} = \frac{1}{4}W_{\alpha v\zeta,\alpha\mu\xi}\left[V_{\mu\xi,v\zeta} + \left(\sum_\rho W_{\mu\xi\rho,v\zeta\rho}n_\rho\right)\right]. \quad (2.22)$$

In Eq. (2.19) the first term is the contribution of the diagrams with 2p-1h in the intermediate processes corresponding to the first four diagrams in Fig. 3, the second term is that of the fifth diagram with 3p-2h in the intermediate process, and the third term is that of the sixth and seventh diagrams with 2p-2h in the intermediate process. There is no time propagation in the sixth and seventh diagrams of Fig. 3. If only two-body interactions exist, then there is only the first diagram in Fig. 3.

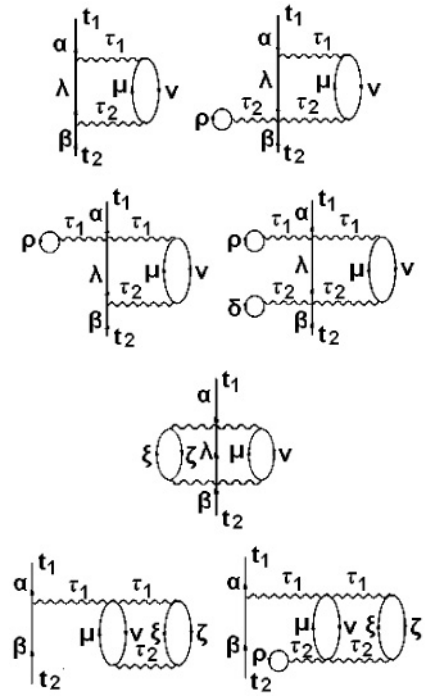

FIG. 3. Second order Feynman diagrams of the one-particle Green functions which cannot be offset by the mean field.

III. FORMULATION OF THE NUCLEON MICROSCOPIC OPTICAL POTENTIAL

In order to simplify the calculation, we use the nuclear matter approach. In the Fermi gas model for symmetric nuclear matter, which has equal numbers of neutrons and protons, the density ρ of the nuclear matter is related to the Fermi momentum k_F by

$$\rho = \frac{2}{3\pi^2}k_F^3. \quad (3.1)$$

The symmetric nuclear matter is the special case of the asymmetric nuclear matter. For asymmetric nuclear matter where the neutrons and protons have different Fermi momentum k_n and k_p, the neutron density ρ_n and proton density ρ_p are expressed by

$$\rho_\tau = \frac{1}{3\pi^2}k_\tau^3, \quad \tau = n \text{ or } p. \quad (3.2)$$

Defining the asymmetric parameter α_0 as

$$\alpha_0 = (\rho_n - \rho_p)/\rho, \quad \rho = \rho_n + \rho_p \quad (3.3)$$

Eq. (3.2) can be written as

$$\rho_n = \tfrac{1}{2}(1+\alpha_0)\rho, \quad \rho_p = \tfrac{1}{2}(1-\alpha_0)\rho \quad (3.4)$$

and

$$k_n = (1+\alpha_0)^{1/3}k_F, \quad k_p = (1-\alpha_0)^{1/3}k_F. \quad (3.5)$$

The Coulomb potential in nuclear matter is expressed as

$$V_C = \frac{3zZe^2}{2R_c}. \tag{3.6}$$

In the nuclear matter the wave function of nucleon α is just the plane wave function

$$\psi_\alpha(\vec{r}) = \frac{1}{\sqrt{\Omega}} e^{i\vec{k}_\alpha\cdot\vec{r}} x_{\sigma_\alpha} x_{\tau_\alpha}, \tag{3.7}$$

where χ_{σ_α} and χ_{τ_α} are the spin and isospin wave functions, respectively, Ω is the volume, spin $\sigma_\alpha = \frac{1}{2}$ or $-\frac{1}{2}$ and isospin $\tau_\alpha = \frac{1}{2}$ (for neutron) or $-\frac{1}{2}$ (for proton).

Our purpose is to investigate the MOP for even-even nuclei with the asymmetric nuclear matter approximation.

The real part of the nucleon MOP is obtained with the first order mass operator based on Eq. (2.15)

$$V_{\tau_\alpha} = M^{(1)}_{\alpha\alpha} = \sum_{\rho\leqslant F} V_{\alpha\rho,\alpha\rho} + \frac{1}{2}\sum_{\rho,\delta\leqslant F} W_{\alpha\rho\delta,\alpha\rho\delta}. \tag{3.8}$$

The summation conditions $\leqslant F$ and $> F$ represent below and above Fermi surfaces, respectively. The second order diagrams are the lowest order diagrams to contribute to the imaginary part of the MOP. That means

$$W_{\tau_\alpha} = \mathrm{Im}\, M^{(2)}_{\alpha\alpha}. \tag{3.9}$$

The formula for the principle value integral is expressed as

$$\frac{1}{x \pm i\varepsilon} = \mathscr{P}\frac{1}{x} \mp i\pi\delta(x). \tag{3.10}$$

Based on the above formula we can see that the sixth and seventh diagrams in Fig. 3 have no contribution to the imaginary part of MOP since $\varepsilon_v + \varepsilon_\zeta - \varepsilon_\mu - \varepsilon_\xi < 0$ in any case. Then from Eq. (2.19) we have

$$W_{\tau_\alpha} = W_A + W_B, \tag{3.11}$$

where

$$W_A = -\pi \sum_{\substack{\lambda,\mu>F\\ v\leqslant F}} A_{\alpha\lambda\mu v\alpha}\delta(\varepsilon_\alpha + \varepsilon_v - \varepsilon_\lambda - \varepsilon_\mu), \tag{3.12}$$

$$W_B = -\pi \sum_{\substack{\lambda,\,\mu,\,\xi\,>\,F\\ v,\,\zeta\,\leqslant F}} B_{\alpha\lambda\mu v\xi\zeta\alpha}\delta(\varepsilon_\alpha + \varepsilon_v + \varepsilon_\zeta - \varepsilon_\lambda - \varepsilon_\mu - \varepsilon_\xi), \tag{3.13}$$

$\varepsilon_\alpha = \omega$ is the incident particle energy. From Eqs. (2.20) and (2.21) $A_{\alpha\lambda\mu v\alpha}$ and $B_{\alpha\lambda\mu v\xi\zeta\alpha}$ are obtained as follows:

$$\begin{aligned} A_{\alpha\lambda\mu v\alpha} &= \frac{1}{2}V_{\alpha v,\lambda\mu}V_{\lambda\mu,\alpha v} + \frac{1}{2}V_{\alpha v,\lambda\mu}\left(\sum_{\rho\leqslant F} W_{\lambda\mu\rho,\alpha v\rho}\right) \\ &\quad + \frac{1}{2}\left(\sum_{\rho\leqslant F} W_{\alpha v\rho,\lambda\mu\rho}\right)V_{\lambda\mu,\alpha v} \\ &\quad + \frac{1}{2}\left(\sum_{\rho\leqslant F} W_{\alpha v\rho,\lambda\mu\rho}\right)\left(\sum_{\delta\leqslant F} W_{\lambda\mu\delta,\alpha v\delta}\right), \end{aligned} \tag{3.14}$$

$$B_{\alpha\lambda\mu v\xi\zeta\alpha} = \frac{1}{12}W_{\alpha v\zeta,\lambda\mu\xi}W_{\lambda\mu\xi,\alpha v\zeta}. \tag{3.15}$$

Based on Eqs. (2.17) and (2.18) the two-body and three-body interaction matrix elements read

$$\begin{aligned} V_{\alpha v,\lambda\mu} &= \langle\psi_\alpha(\vec{r}_1)\psi_v(\vec{r}_2)|V_{12}(\vec{R},\vec{r})|(\psi_\lambda(\vec{r}_1)\psi_\mu(\vec{r}_2) \\ &\quad - \psi_\mu(\vec{r}_1)\psi_\lambda(\vec{r}_2))\rangle, \end{aligned} \tag{3.16}$$

$$\begin{aligned} W_{\alpha v\zeta,\lambda\mu\xi} &= \langle\psi_\alpha(\vec{r}_1)\psi_v(\vec{r}_2)\psi_\zeta(\vec{r}_3)|W_{123} \\ &\quad \times(\vec{r}_1,\vec{r}_2,\vec{r}_3)\left|\sum_p (-)^p\psi_\lambda(\vec{r}_1)\psi_\mu(\vec{r}_2)\psi_\xi(\vec{r}_3)\right\rangle, \end{aligned} \tag{3.17}$$

where $|\sum_p\cdots\rangle$ means antisymmetrization. Note the state number of phase space in nuclear matter is

$$\sum_{\tau\sigma}\frac{\Omega\int \mathrm{d}\vec{p}}{(2\pi\hbar)^3} = \sum_{\tau\sigma}\frac{\Omega\int \mathrm{d}\vec{k}}{(2\pi)^3}. \tag{3.18}$$

The summations to spin and isispin are included in the above expression. Putting Eqs. (2.5), (2.4), (3.7) into Eqs. (3.16), (3.17), (3.8) and using the following formulas:

$$\frac{1}{(2\pi)^3}\int e^{i\vec{k}\cdot\vec{r}}\,\mathrm{d}\vec{r} = \delta(\vec{k}), \tag{3.19}$$

$$\frac{1}{\Omega}\int \mathrm{d}\vec{r} = 1, \quad \rho_{\tau_\alpha} = N_{\tau_\alpha}/\Omega, \tag{3.20}$$

$$\vec{\sigma} = \sum_p (-)^p\sigma_p\vec{e}_{-p} = \sum_p \sigma_p\vec{e}^{\,*}_p, \tag{3.21}$$

$$\begin{aligned} J_\mu|jm\rangle &= \sqrt{j(j+1)}C^{j\,\mathrm{m}+\mu}_{jm\,1\mu}|j\,m+\mu\rangle, \\ \sigma_p x_\mu &= \sqrt{3}C^{\frac{1}{2}\mu+p}_{\frac{1}{2}\mu\,1p}x_{\mu+p}, \end{aligned} \tag{3.22}$$

where N_{τ_α} is the number of nucleon τ_α below Fermi surface, the real part of the nucleon MOP for even-even nucleus are obtained as follows:

$$\begin{aligned} V_{\tau_\alpha} &= t_0\left[\left(1+\frac{x_0}{2}\right)\rho - \left(x_0+\frac{1}{2}\right)\rho_{\tau_\alpha}\right] \\ &\quad + \frac{1}{6}t_3\rho^\alpha\left[\left(1+\frac{x_3}{2}\right)\rho - \left(x_3+\frac{1}{2}\right)\rho_{\tau_\alpha}\right] \\ &\quad + \frac{1}{4}t_{03}\left(\rho^2 - \rho^2_{\tau_\alpha}\right) \\ &\quad + \frac{1}{4}\left\{t_1\left[\left(1+\frac{x_1}{2}\right)\rho - \left(x_1+\frac{1}{2}\right)\rho_{\tau_\alpha}\right]\right. \\ &\quad + t_4\rho\left[\left(1+\frac{x_4}{2}\right)\rho - \left(x_4+\frac{1}{2}\right)\rho_{\tau_\alpha}\right] \\ &\quad + t_2\left[\left(1+\frac{x_2}{2}\right)\rho + \left(x_2+\frac{1}{2}\right)\rho_{\tau_\alpha}\right] \\ &\quad \left.+ t_5\rho\left[\left(1+\frac{x_5}{2}\right)\rho + \left(x_5+\frac{1}{2}\right)\rho_{\tau_\alpha}\right]\right\}k^2_\alpha \\ &\quad + \frac{1}{40\pi^2}\{[t_1(1-x_1) + t_4\rho(1-x_4) + 3t_2(1+x_2) \\ &\quad + 3t_5\rho(1+x_5)]k^5_{\tau_\alpha} + [t_1(2+x_1) + t_4\rho(2+x_4) \\ &\quad + t_2(2+x_2) + t_5\rho(2+x_5)]k^5_{-\tau_\alpha}\}, \end{aligned} \tag{3.23}$$

where k_{τ_α} is the Fermi momentum of the nucleon τ_α. From the above expression we can see that the W_0 term of Skyrme force

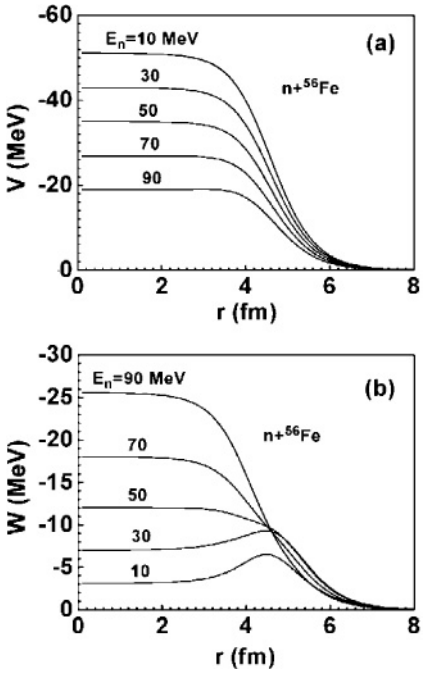

FIG. 4. Radial dependence of the neutron MOP for ^{56}Fe at energies 10–90 MeV. The curves are the theoretical values computed with GS2. (a) The real parts. (b) The imaginary parts.

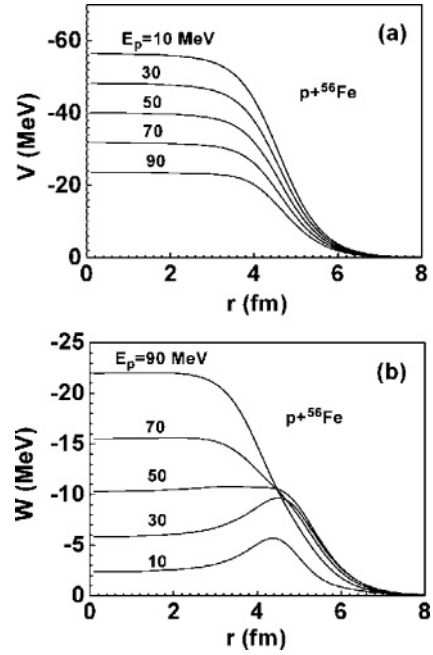

FIG. 5. Radial dependence of the proton MOP for ^{56}Fe at energies 10–90 MeV. The curves are the theoretical values computed with GS2. (a) The real parts. (b) The imaginary parts.

has no contribution to the real part of nucleon MOP. Then the nucleon effective mass m^* can be obtained as follows:

$$\frac{m^*_{\tau_\alpha}}{m_{\tau_\alpha}} = \left\{1 + \frac{m_{\tau_\alpha}}{2\hbar^2}\left\{t_1\left[\left(1+\frac{x_1}{2}\right)\rho - \left(x_1+\frac{1}{2}\right)\rho_{\tau_\alpha}\right] + t_4\rho\left[\left(1+\frac{x_4}{2}\right)\rho - \left(x_4+\frac{1}{2}\right)\rho_{\tau_\alpha}\right] + t_2\left[\left(1+\frac{x_2}{2}\right)\rho + \left(x_2+\frac{1}{2}\right)\rho_{\tau_\alpha}\right] + t_5\rho\left[\left(1+\frac{x_5}{2}\right)\rho + \left(x_5+\frac{1}{2}\right)\rho_{\tau_\alpha}\right]\right\}\right\}^{-1}, \tag{3.24}$$

where k_α^2 is given by

$$k_\alpha^2 = \frac{2m_{\tau_\alpha}}{\hbar^2}\left(\frac{M}{M+m_{\tau_\alpha}}E_L - V_{\tau_\alpha} - V_C\right) \tag{3.25}$$

and m_{τ_α} and M are the mass of the nucleon τ_α and the target nucleus, respectively. E_L is the energy of the incident nucleon in the laboratory frame. V_C is the Coulomb potential. Then we have

$$V_{\tau_\alpha} = \frac{m^*_{\tau_\alpha}}{m_{\tau_\alpha}}\left\{t_0\left[\left(1+\frac{x_0}{2}\right)\rho - \left(x_0+\frac{1}{2}\right)\rho_{\tau_\alpha}\right] + \frac{t_3}{6}\rho^\alpha\left[\left(1+\frac{x_3}{2}\right)\rho - \left(x_3+\frac{1}{2}\right)\rho_{\tau_\alpha}\right] + \frac{t_{03}}{4}\left(\rho^2-\rho_{\tau_\alpha}^2\right) + \frac{1}{4}\left\{t_1\left[\left(1+\frac{x_1}{2}\right)\rho - \left(x_1+\frac{1}{2}\right)\rho_{\tau_\alpha}\right] + t_4\rho\left[\left(1+\frac{x_4}{2}\right)\rho - \left(x_4+\frac{1}{2}\right)\rho_{\tau_\alpha}\right] + t_2\left[\left(1+\frac{x_2}{2}\right)\rho + \left(x_2+\frac{1}{2}\right)\rho_{\tau_\alpha}\right] + t_5\rho\left[\left(1+\frac{x_5}{2}\right)\rho + \left(x_5+\frac{1}{2}\right)\rho_{\tau_\alpha}\right]\right\} \times \frac{2m_{\tau_\alpha}}{\hbar^2}\left(\frac{M}{M+m_{\tau_\alpha}}E_L - V_C\right) + \frac{1}{40\pi^2}\{[t_1(1-x_1) + t_4\rho(1-x_4) + 3t_2(1+x_2) + 3t_5\rho(1+x_5)]k_{\tau_\alpha}^5 + [t_1(2+x_1) + t_4\rho(2+x_4) + t_2(2+x_2) + t_5\rho(2+x_5)]k_{-\tau_\alpha}^5\}. \tag{3.26}$$

This expression shows that the real part of the nucleon MOP has a linear relation with E_L and is isospin dependent.

By using Eq. (3.19) the following relations can be proved:

$$\frac{(2\pi)^3}{\Omega^2}\delta(\vec{k}_\lambda + \vec{k}_\mu - \vec{k}_\alpha - \vec{k}_v)\frac{(2\pi)^3}{\Omega^2}\delta(\vec{k}_\alpha + \vec{k}_v - \vec{k}_\lambda - \vec{k}_\mu) = \frac{(2\pi)^3}{\Omega^3}\delta(\vec{k}_\alpha + \vec{k}_v - \vec{k}_\lambda - \vec{k}_\mu), \tag{3.27}$$

$$\frac{(2\pi)^3}{\Omega^3}\delta(\vec{k}_\lambda + \vec{k}_\mu + \vec{k}_\xi - \vec{k}_\alpha - \vec{k}_v - \vec{k}_\zeta) \times \frac{(2\pi)^3}{\Omega^3}\delta(\vec{k}_\alpha + \vec{k}_v + \vec{k}_\zeta - \vec{k}_\lambda - \vec{k}_\mu - \vec{k}_\xi) = \frac{(2\pi)^3}{\Omega^5}\delta(\vec{k}_\alpha + \vec{k}_v + \vec{k}_\zeta - \vec{k}_\lambda - \vec{k}_\mu - \vec{k}_\xi). \tag{3.28}$$

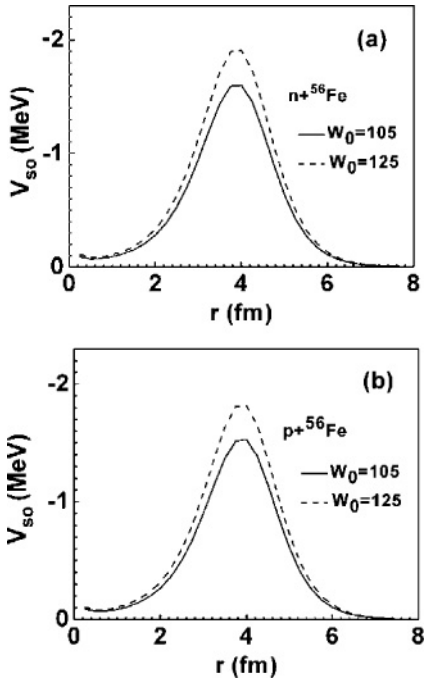

FIG. 6. Radial dependence of the real parts of the spin-orbit potential for ^{56}Fe. The curves are the theoretical values computed with $W_0 = 105$ and 125. (a) Neutron. (b) Proton.

Putting Eqs. (2.5), (2.4), and (3.7) into Eqs. (3.11)–(3.17) and using the following formulas:

$$\vec{A} = \sum_p (-)^p A_p \vec{e}_{-p} = \sum_p A_p \vec{e}^{\,*}_p, \quad \vec{e}^{\,*}_p \cdot \vec{e}_{p'} = \delta_{pp'}, \quad (3.29)$$

$$V_{\tau_\alpha} = V_0 + bk_\alpha^2, \quad \varepsilon_\alpha = \frac{\hbar^2 k_\alpha^2}{2m} + V_{\tau_\alpha} = \frac{\hbar^2 k_\alpha^2}{2m^*_{\tau_\alpha}} + V_0, \quad (3.30)$$

the imaginary part of the nucleon MOP for the even-even nucleus are obtained as follows:

$$W_A = -\frac{\pi}{(2\pi)^6} \sum_{i=1}^{7} W_i, \quad (3.31)$$

$$W_B = -\frac{\pi}{(2\pi)^{12}} W_T, \quad (3.32)$$

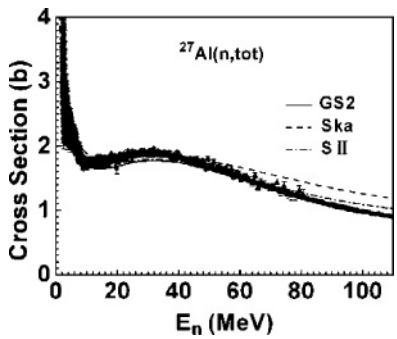

FIG. 7. Calculated neutron total cross sections compared with experimental data [36–38] for $n + {}^{27}$Al reaction. The theoretical values computed with GS2 are shown as the solid curve, those computed with Ska are shown as the dashed curve, and those computed with SII are shown as the dot-dashed curve.

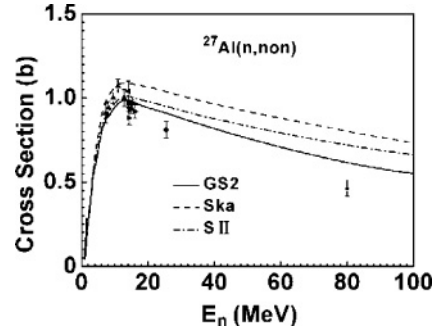

FIG. 8. Calculated neutron nonelastic cross sections compared with experimental data [39–45] for $n + {}^{27}$Al reaction. The theoretical values computed with GS2 are shown as the solid curve, those computed with Ska are shown as the dashed curve, and those computed with SII are shown as the dot-dashed curve.

where

$$\begin{aligned}
W_1 = {} & \big[2\big(1 + x_0 + x_0^2\big)t_0^2 + \tfrac{1}{18}\big(1 + x_3 + x_3^2\big)t_3^2\rho^{2\alpha} \\
& + \tfrac{1}{3}(2 + x_0 + x_3 + 2x_0x_3)t_0t_3\rho^{\alpha} \\
& + (2 + x_0)t_0t_{03}\rho + \tfrac{1}{6}(2 + x_3)t_0t_{03}\rho^{1+\alpha} + \tfrac{1}{2}t_{03}^2\rho^2\big] \\
& \times [I_1(\tau_\alpha, \tau_\alpha) + I_1(\tau_\alpha, -\tau_\alpha)] \\
& - \big[\big(1 + 4x_0 + x_0^2\big)t_0^2 + \tfrac{1}{36}\big(1 + 4x_3 + x_3^2\big)t_3^2\rho^{2\alpha} \\
& + \tfrac{1}{3}(1 + 2x_0 + 2x_3 + x_0x_3)t_0t_3\rho^{\alpha} + (1 + 2x_0)t_0t_{03}\rho \\
& + \tfrac{1}{6}(1 + 2x_3)t_3t_{03}\rho^{1+\alpha} + \tfrac{1}{4}t_{03}^2\rho^2\big]I_1(\tau_\alpha, \tau_\alpha), \quad (3.33)
\end{aligned}$$

$$\begin{aligned}
W_2 = {} & \tfrac{1}{2}\big[(2 + x_0 + x_1 + 2x_0x_1)t_0t_1 \\
& + (2 + x_0 + x_4 + 2x_0x_4)t_0t_4\rho \\
& + \tfrac{1}{6}(2 + x_3 + x_1 + 2x_3x_1)t_3t_1\rho^{\alpha} \\
& + \tfrac{1}{6}(2 + x_3 + x_4 + 2x_3x_4)t_3t_4\rho^{1+\alpha} \\
& + \tfrac{1}{2}(2 + x_1)t_1t_{03}\rho + \tfrac{1}{2}(2 + x_4)t_4t_{03}\rho^2\big] \\
& \times [I_2(\tau_\alpha, \tau_\alpha) + I_2(\tau_\alpha, -\tau_\alpha)] \\
& - \tfrac{1}{2}\big[(1 + 2x_0 + 2x_1 + x_0x_1)t_0t_1 \\
& + (1 + 2x_0 + 2x_4 + x_0x_4)t_0t_4\rho \\
& + \tfrac{1}{6}(1 + 2x_3 + 2x_1 + x_3x_1)t_3t_1\rho^{\alpha} \\
& + \tfrac{1}{6}(1 + 2x_3 + 2x_4 + x_3x_4)t_3t_4\rho^{1+\alpha} \\
& + \tfrac{1}{2}(1 + 2x_1)t_{03}t_1\rho \\
& + \tfrac{1}{2}(1 + 2x_4)t_{03}t_4\rho^2\big]I_2(\tau_\alpha, \tau_\alpha), \quad (3.34)
\end{aligned}$$

$$\begin{aligned}
W_3 = {} & \tfrac{1}{8}\big[\big(1 + x_1 + x_1^2\big)t_1^2 + \big(1 + x_4 + x_4^2\big)t_4^2\rho^2 \\
& + (2 + x_1 + x_4 + 2x_1x_4)t_1t_4\rho\big]\big[I_3(\tau_\alpha, \tau_\alpha) \\
& + I_3(\tau_\alpha, -\tau_\alpha)\big] - \tfrac{1}{16}\big[\big(1 + 4x_1 + x_1^2\big)t_1^2 \\
& + \big(1 + 4x_4 + x_4^2\big)t_4^2\rho^2 + 2(1 + 2x_1 + 2x_4 \\
& + x_1x_4)t_1t_4\rho\big]I_3(\tau_\alpha, \tau_\alpha), \quad (3.35)
\end{aligned}$$

$$\begin{aligned}
W_4 = {} & \tfrac{1}{2}\big[(2 + x_0 + x_2 + 2x_0x_2)t_0t_2 \\
& + (2 + x_0 + x_5 + 2x_0x_5)t_0t_5\rho \\
& + \tfrac{1}{6}(2 + x_3 + x_2 + 2x_3x_2)t_3t_2\rho^{\alpha} \\
& + \tfrac{1}{6}(2 + x_3 + x_5 + 2x_3x_5)t_3t_5\rho^{1+\alpha} \\
& + \tfrac{1}{2}(2 + x_2)t_{03}t_2\rho + \tfrac{1}{2}(2 + x_5)t_{03}t_5\rho^2\big]I_4(\tau_\alpha, -\tau_\alpha), \\
& \quad (3.36)
\end{aligned}$$

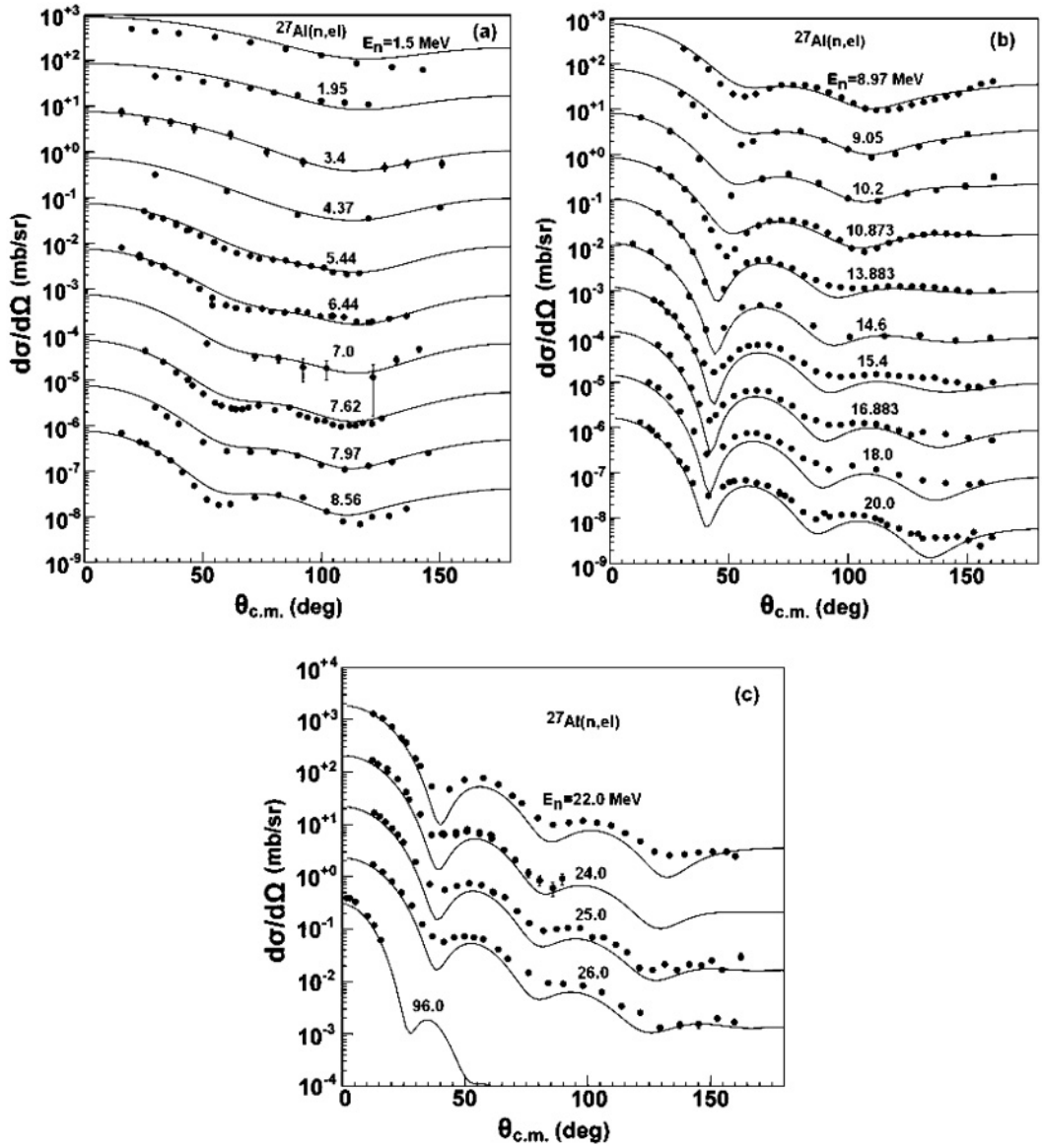

FIG. 9. Calculated neutron elastic scattering angular distributions (solid line) compared with experimental data [46–57] for $n + {}^{27}\mathrm{Al}$ reaction. The results are offset by factors of 10.

$$\begin{aligned} W_5 = {} & \tfrac{1}{8}\big[(2 + x_1 + x_2 + 2x_1x_2)t_1t_2 \\ & + (2 + x_1 + x_5 + 2x_1x_5)t_1t_5\rho \\ & + (2 + x_4 + x_2 + 2x_4x_2)t_4t_2\rho \\ & + (2 + x_4 + x_5 + 2x_4x_5)t_4t_5\rho^2\big]I_5(\tau_\alpha, -\tau_\alpha), \end{aligned} \tag{3.37}$$

$$\begin{aligned} W_6 = {} & \tfrac{1}{8}\big[\big(1 + x_2 + x_2^2\big)t_2^2 + \big(1 + x_5 + x_5^2\big)t_5^2\rho^2 \\ & + (2 + x_2 + x_5 + 2x_2x_5)t_2t_5\rho\big] \\ & \times [I_6(\tau_\alpha, \tau_\alpha) + I_6(\tau_\alpha, -\tau_\alpha)] + \tfrac{1}{16}\big[\big(1 + 4x_2 + x_2^2\big)t_2^2 \\ & + \big(1 + 4x_5 + x_5^2\big)t_5^2\rho^2 + 2(1 + 2x_2 \\ & + 2x_5 + x_2x_5)t_2t_5\rho\big]I_6(\tau_\alpha, \tau_\alpha), \end{aligned} \tag{3.38}$$

$$W_7 = \tfrac{1}{4}W_0^2[2I_7(\tau_\alpha, \tau_\alpha) + I_7(\tau_\alpha, -\tau_\alpha)], \tag{3.39}$$

$$W_T = t_{03}^2[2I_B(\tau_\alpha, \tau_\alpha, -\tau_\alpha) + I_B(\tau_\alpha, -\tau_\alpha, -\tau_\alpha)], \tag{3.40}$$

$$I_i(\tau_\alpha, \tau_\nu) \equiv I_i(\tau_\alpha\tau_\nu\tau_\alpha\tau_\nu), \quad i = 1 \sim 7, \tag{3.41}$$

$$I_B(\tau_\alpha, \tau_\nu, \tau_\zeta) \equiv I_B(\tau_\alpha\tau_\nu\tau_\zeta\tau_\alpha\tau_\nu\tau_\zeta) \tag{3.42}$$

$$\begin{aligned} I_i(\tau_\alpha\tau_\nu\tau_\alpha\tau_\nu) = {} & \int \mathrm{d}\vec{k}_\nu \mathrm{d}\vec{k}_\lambda \mathrm{d}\vec{k}_\mu f_i(\vec{k}_{\alpha\nu}, \vec{k}_{\lambda\mu}) \\ & \times \delta(\vec{k}_\alpha + \vec{k}_\nu - \vec{k}_\lambda - \vec{k}_\mu) \\ & \times \delta(\varepsilon_\alpha + \varepsilon_\nu - \varepsilon_\lambda - \varepsilon_\mu), \quad i = 1 \sim 7, \end{aligned} \tag{3.43}$$

$$\begin{aligned} & f_1 = 1, \quad f_2 = \tfrac{1}{2}\big(k_{\alpha\nu}^2 + k_{\lambda\mu}^2\big), \\ & f_3 = \tfrac{1}{4}\big(k_{\alpha\nu}^2 + k_{\lambda\mu}^2\big)^2, \quad f_4 = \vec{k}_{\alpha\nu} \cdot \vec{k}_{\lambda\mu}, \\ & f_5 = \tfrac{1}{2}\big(k_{\alpha\nu}^2 + k_{\lambda\mu}^2\big)(\vec{k}_{\alpha\nu} \cdot \vec{k}_{\lambda\mu}), \\ & f_6 = \tfrac{1}{2}(\vec{k}_{\alpha\nu} \cdot \vec{k}_{\lambda\mu})^2, \quad f_7 = (\vec{k}_{\alpha\nu} \times \vec{k}_{\lambda\mu})^2, \end{aligned} \tag{3.44}$$

$$\vec{k}_{\alpha\nu} \equiv \vec{k}_\alpha - \vec{k}_\nu, \quad \vec{k}_{\lambda\mu} \equiv \vec{k}_\lambda - \vec{k}_\mu$$
$$I_B(\tau_\alpha\tau_\nu\tau_\zeta\tau_\alpha\tau_\nu\tau_\zeta) = \int \mathrm{d}\vec{k}_\nu \mathrm{d}\vec{k}_\zeta \mathrm{d}\vec{k}_\lambda \mathrm{d}\vec{k}_\mu \mathrm{d}\vec{k}_\xi \times \delta(\vec{k}_\alpha + \vec{k}_\nu + \vec{k}_\zeta - \vec{k}_\lambda - \vec{k}_\mu - \vec{k}_\xi) \times \delta(\varepsilon_\alpha + \varepsilon_\nu + \varepsilon_\zeta - \varepsilon_\lambda - \varepsilon_\mu - \varepsilon_\xi). \tag{3.45}$$

The integral I_B is for three-body force only. In the above integrals the condition $\nu, \varsigma \leqslant F$ and $\alpha, \lambda, \mu, \xi > F$ must be satisfied. $\hbar\vec{k}_\alpha$ is the incident nucleon momentum. For asymmetric nuclear matter the integrals (3.43) and (3.45) are provided in Appendixes A and B, respectively.

The simplest way to obtain MOP for a finite nucleus is to use the LDA [33]. We assume that the densities of the neutrons and protons in a spherical nucleus have the same geometrical distributions and are expressed by Negele's empirical formula

$$\rho_\tau(r) = \frac{\rho_{0\tau}}{1 + \exp[(r-c)/a]}, \quad \tau = n \quad \text{or} \quad p, \tag{3.46}$$

where

$$\rho_{0\tau} = \frac{3N_\tau}{4\pi c^3(1 + \pi^2 a^2/c^2)},$$
$$N_\tau = \begin{cases} N & \text{for} \quad \tau = n \\ Z & \text{for} \quad \tau = p \end{cases}, \tag{3.47}$$
$$c = (0.978 + 0.0206A^{1/3})A^{1/3}, \quad a = 0.54. \tag{3.48}$$

In this case the asymmetric parameter can be deduced as

$$\alpha_0 = (N - Z)/A. \tag{3.49}$$

In general the optical potential has the following form:

$$U_{\tau_\alpha}(r) = V_{\tau_\alpha}(r) + iW_{\tau_\alpha}(r) + \left[V_{\mathrm{so}}^{\tau_\alpha}(r) + iW_{\mathrm{so}}^{\tau_\alpha}(r)\right](\vec{\sigma}\cdot\vec{l}). \tag{3.50}$$

However, we only have $V_{\tau_\alpha}(r)$ and $W_{\tau_\alpha}(r)$ without spin-orbit parts $V_{\mathrm{so}}^{\tau_\alpha}(r)$ and $W_{\mathrm{so}}^{\tau_\alpha}(r)$ which, as is known, vanish in nuclear matter. In order to get the spin-orbit term, we start from the HF calculation for the finite nuclei. In the HF calculation of the spherical nuclei, for the extended Skyrme force, the spin-orbit term of the real part is expressed as [17]

$$V_{\mathrm{so}}^{\tau_\alpha}(r) = \frac{1}{2}W_0\frac{1}{r}\frac{d}{dr}[\rho(r) + \rho_{\tau_\alpha}(r)] - \frac{1}{8r}[t_1x_1 + t_2x_2 + t_4x_4\rho(r) + t_5x_5\rho(r)]J(r) + \frac{1}{8r}[t_1 - t_2 + t_4\rho(r) - t_5\rho(r)]J_{\tau_\alpha}(r), \tag{3.51}$$

where $J_{\tau_\alpha}(r)$ is the spin density. The numerical result [15,34] show that the contribution of the term produced by the central force involving $J_{\tau_\alpha}(r)$ is much smaller than the first term directly arising from the two-body spin-orbit force W_0. Thus we only keep the first term and Eq. (3.51) can be reduced to

$$V_{\mathrm{so}}^{\tau_\alpha}(r) = \frac{1}{2}W_0\frac{1}{r}\frac{d}{dr}[\rho(r) + \rho_{\tau_\alpha}(r)], \tag{3.52}$$

where $\rho(r)$ and $\rho_{\tau_\alpha}(r)$ are described by Negele's empirical formula (3.46) as before. Then Eq. (3.52) is an analytical expression.

The imaginary part of the spin-orbit potential $W_{\mathrm{so}}^{\tau_\alpha}(r)$ below 100 MeV is usually very small, which is often omitted. Its contribution to MOP is also omitted here.

Above, the nucleon MOP formulas are derived for the even-even nucleus. We know that in the nuclear matter approach the average effect of the nucleus is studied. For heavier nuclei, the difference between the nucleus with one more neutron or one more proton than the even-even nucleus is small and the difference between the nucleus with the spin up or spin down neutron (or proton) is also small, so we could take their average value. Therefore, the MOP obtained above can be applied to the odd-even nucleus approximately. Similarly, the difference between the nucleus with the unpaired neutron or unpaired proton is small, so we could take their average value. Therefore, the MOP obtained above can be applied to the odd-odd nucleus approximately too. In principle the MOP obtained above can be applied to all nuclei which are not too light and the real N, Z, A of the target nucleus should be used in calculations.

IV. RESULTS AND ANALYSES

Firstly, we use the conventional Skyrme forces SII-SVI to calculate the MOP. In certain energy regions the calculated MOP are in reasonable agreement with the phenomenological optical potential (POP) [35] and the MOP based on the BHF approximation [3]. Comparing the results calculated with five sets of parameters SII–SVI, we have found that the real part of the MOP calculated with SIII is the best, but the imaginary parts of such are poor, because its energy dependence rises too steeply. Considering both the real and the imaginary parts as a whole it seems that the MOP with SII is the best one. In addition, there also appear some shortcomings in the MOP calculated with the conventional Skyrme forces. For example, the surface region of the real parts in the low energy region has the unnecessary peak; the depths of the real parts are smaller; energy variation of the imaginary parts is too fast, etc. We come to use the extended Skyrme forces ($t_{03} = 0$) to

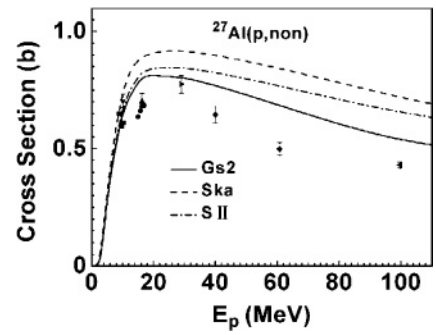

FIG. 10. Calculated reaction cross sections compared with experimental data [58–63] for $p + {}^{27}$Al reaction. The theoretical values computed with GS2 are shown as the solid curve, those computed with Ska are shown as the dashed curve, and those computed with SII are shown as the dot-dashed curve.

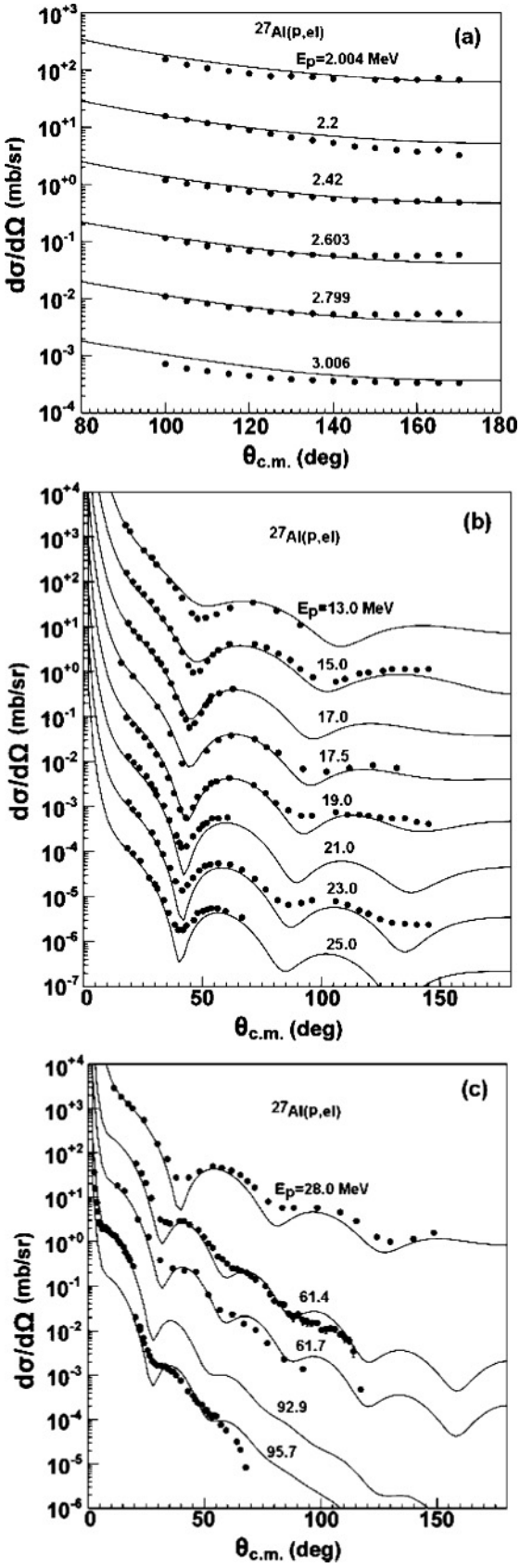

FIG. 11. Calculated elastic scattering angular distributions (solid line) compared with experimental data [64–70] for $p + {}^{27}\mathrm{Al}$ reaction. The results are offset by factors of 10.

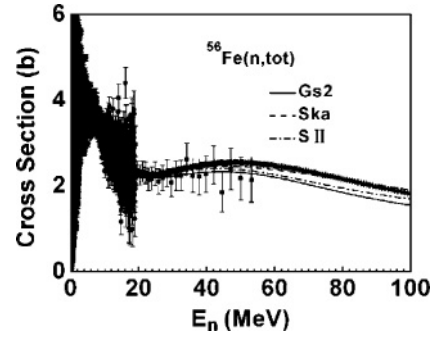

FIG. 12. Calculated neutron total cross sections compared with experimental data [71–73] for $n + {}^{56}\mathrm{Fe}$ reaction. The theoretical values computed with GS2 are shown as the solid curve, those computed with Ska are shown as the dashed curve, and those computed with SII are shown as the dot-dashed curve.

calculate MOP to test whether this kind of Skyrme force can improve the results. The calculations show that with the extended Skyrme forces many shortcomings due to the conventional Skyrme forces can indeed be overcome, and the agreements with the empirical data have obviously been improved. The results by GS1–GS3 are all quite good, among which the GS2 is the best one. We also show that the calculated results by Ska and Skb are better. In the following presentation, we just show the comparison of the calculation results of cross sections by GS2, Ska, and SII and the angular distributions by GS2 with experimental data for targets ${}^{27}\mathrm{Al}$, ${}^{56}\mathrm{Fe}$, and ${}^{208}\mathrm{Pb}$.

In Figs. 4 and 5 the real and imaginary parts of the neutron and proton MOP for ${}^{56}\mathrm{Fe}$ in the energy range of $E =$ 10–90 MeV computed with GS2 are illustrated. The imaginary part of the MOP changes from the dominant surface absorption into the volume absorption as energy increase as expected from the POP. From the figures above we can also see that the real parts of proton MOP are deeper and the imaginary parts of the proton MOP are shallower than the neutron MOP, especially for low energy and at the surface region of the target nucleus. In other words, the absorption of the protons is less than neutrons.

Figure 6 shows the real parts of the neutron and proton spine-orbit potential for ${}^{56}\mathrm{Fe}$ calculated by Eq. (3.52) with

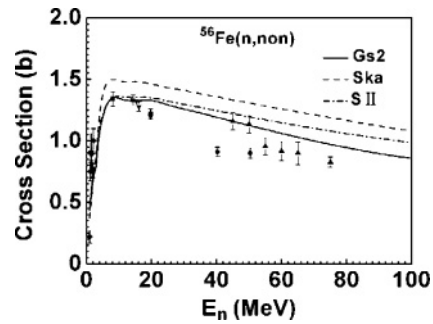

FIG. 13. Calculated neutron nonelastic cross sections compared with experimental data [45,74–76] for $n + {}^{56}\mathrm{Fe}$ reaction. The theoretical values computed with GS2 are shown as the solid curve, those computed with Ska are shown as the dashed curve, and those computed with SII are shown as the dot-dashed curve.

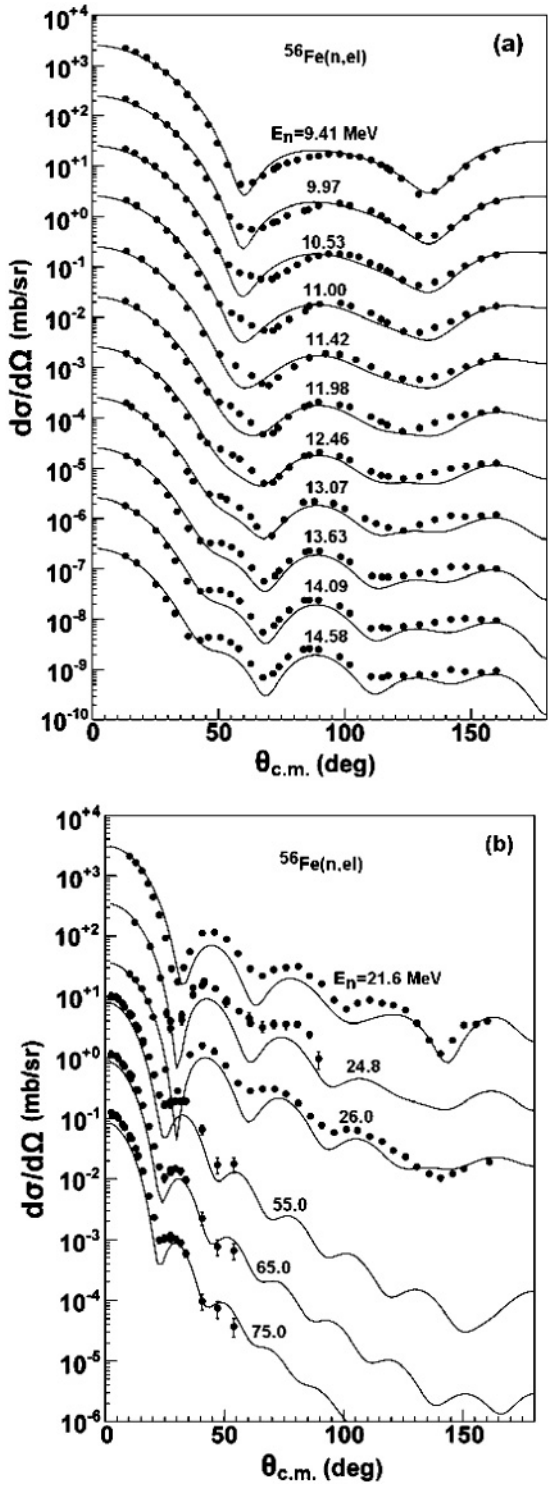

FIG. 14. Calculated elastic scattering angular distributions (solid line) compared with experimental data [77–79] for $n + {}^{56}$Fe reaction. The results are offset by factors of 10.

$W_0 = 105$ and $W_0 = 125$. Their shape and value are reasonable.

The comparisons of calculated results of neutron total and nonelastic cross sections with experimental data for ^{27}Al are given in Figs. 7 and 8. The calculated neutron total cross sections computed with GS2 are in good agreement with the experimental data [36–38] except those for the incident energy from 20 to 40 MeV where the present results are lower than experimental data. The calculated neutron total cross section computed with Ska is in good agreement with the experimental data for the incident energy below 55 MeV, where for higher energies, the magnitudes are larger than the experimental data. As shown in Fig. 8, the shape of calculated neutron nonelastic cross sections computed with GS2, SII and Ska are similar to experimental data [39–45], while the calculated results by GS2 and SII are better in fitting the experimental data for the incident energy below 20 MeV. And the calculated result by GS2 agrees with the trend of experimental data even more.

The calculated neutron elastic scattering angular distributions for ^{27}Al at incident energies from 1.5 to 96.0 MeV are compared with experimental data [46–57] in Fig. 9, the theoretical calculated results are in reasonable agreement with experimental data.

The comparison of calculated results of proton reaction cross sections with experimental data [58–63] for ^{27}Al is given in Fig. 10. The shape of calculated proton reaction cross sections computed with GS2, SII, and Ska are similar to experimental data, while the values for the incident energy below 10 MeV are in reasonable agreement with experimental data. For the higher energies, the calculated values are larger than the experimental data.

The calculated proton elastic scattering angular distributions for ^{27}Al at incident energies from 2.004 to 95.7 MeV are compared with experimental data [64–70] in Fig. 11, the theoretical calculated results are in reasonable agreement with experimental data.

The comparisons of calculated results of neutron total and nonelastic cross sections for ^{56}Fe with experimental data are given in Figs. 12 and 13. As shown in Fig. 12, the calculated neutron total cross section computed with Ska is in reasonable agreement with the experimental data for natural iron taken from Ref. [73], while the calculated result computed with GS2 is in good agreement with the experimental data for the nuclide of ^{56}Fe taken from Refs. [71,72]. As shown in Fig. 13, the calculated nonelastic cross sections by GS2 is in reasonable agreement with the experimental data [45,74–76]

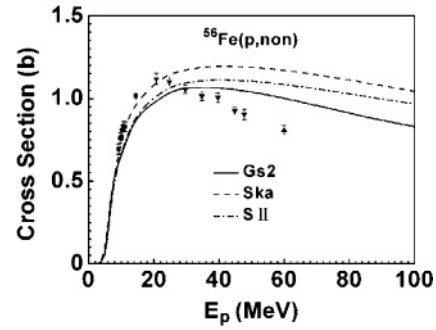

FIG. 15. Calculated proton reaction cross sections compared with experimental data [58,80–82] for $p + {}^{56}$Fe reaction. The theoretical values computed with GS2 are shown as the solid curve, those computed with Ska are shown as the dashed curve, and those computed with SII are shown as the dot-dashed curve.

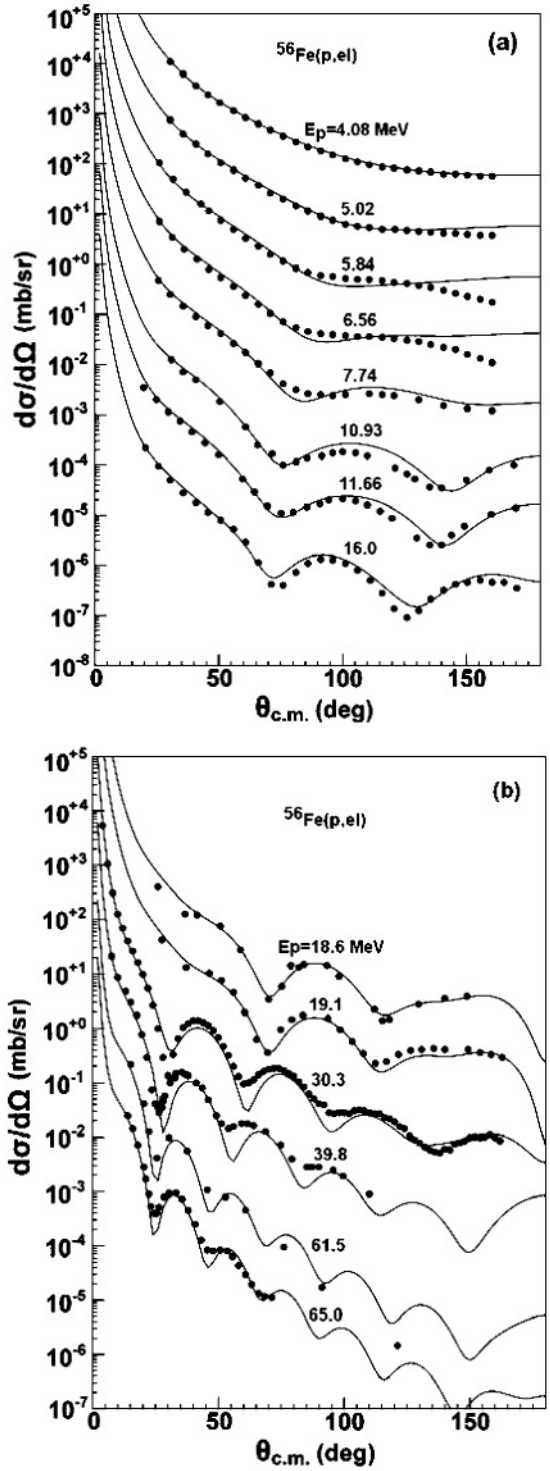

FIG. 16. Calculated elastic scattering angular distributions (solid line) compared with experimental data [69,83–90] for $p + {}^{56}$Fe reaction. The results are offset by factors of 10.

for the incident energy below 55 MeV, where for the higher energies, the calculated magnitudes are larger than the experimental data. And the calculated result by GS2 is better in fitting the experimental data than those by Ska and SII.

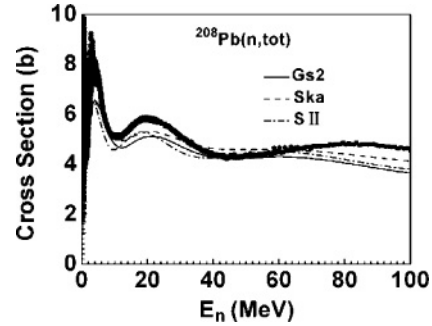

FIG. 17. Calculated neutron total cross sections compared with experimental data [36,91] for $n + {}^{208}$Pb reaction. The theoretical values computed with GS2 are shown as the solid curve, those computed with Ska are shown as the dashed curve, and those computed with SII are shown as the dot-dashed curve.

The calculated neutron elastic scattering angular distributions for ^{56}Fe at incident energies from 9.41 to 75.0 MeV are compared with experimental data [77–79] in Fig. 14, the theoretical calculated results are in reasonable agreement with experimental data.

The comparison of calculated results of proton reaction cross sections with experimental data [58,80–82] for ^{56}Fe is given in Fig. 15. The trend of the calculated results by GS2, SII, and Ska are similar to experimental data, but only the calculated values by Ska for the incident energy below 25 MeV are in reasonable agreement with experimental data.

The calculated proton elastic scattering angular distributions for ^{56}Fe at incident energies from 4.08 to 65.0 MeV are compared with experimental data [69,83–90] in Fig. 16, the theoretical calculated results are in good agreement with experimental data.

The comparisons of calculated results of neutron total and nonelastic cross sections for ^{208}Pb with experimental data are given in Figs. 17 and 18. As shown in Fig. 17, the shapes of calculated neutron total cross section computed with GS2, Ska, and SII are similar to those of the experimental data [36,91], but the values are inconsistent with the experimental data. In Fig. 18, it can be seen that the calculated nonelastic cross sections by GS2 is in reasonable agreement with the experimental

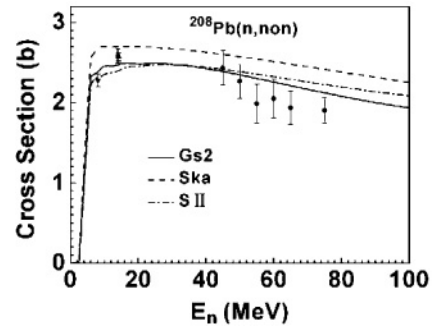

FIG. 18. Calculated neutron nonelastic cross sections compared with experimental data [42,74,92] for $n + {}^{208}$Pb reaction. The theoretical values computed with GS2 are shown as the solid curve, those computed with Ska are shown as the dashed curve, and those computed with SII are shown as the dot-dashed curve.

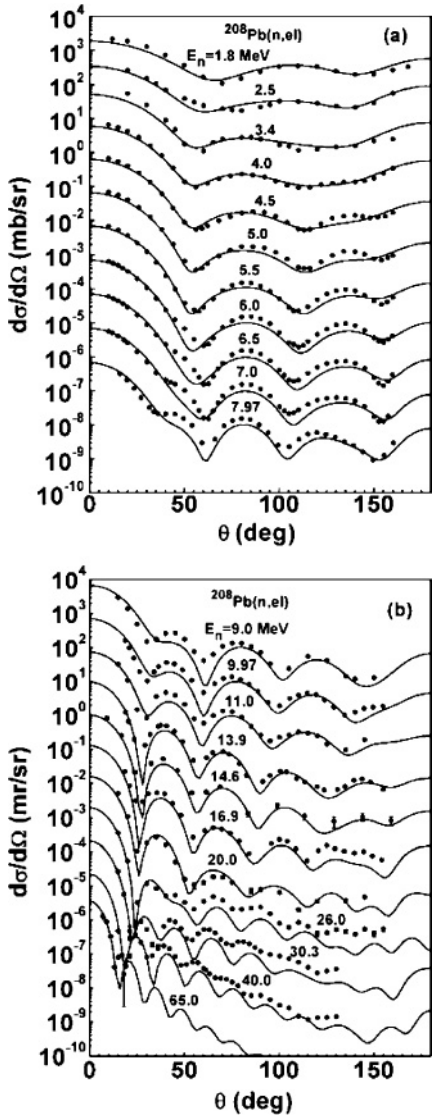

FIG. 19. Calculated elastic scattering angular distributions (solid line) compared with experimental data [54,93–99] for $n + {}^{208}$Pb reaction. The results are offset by factors of 10.

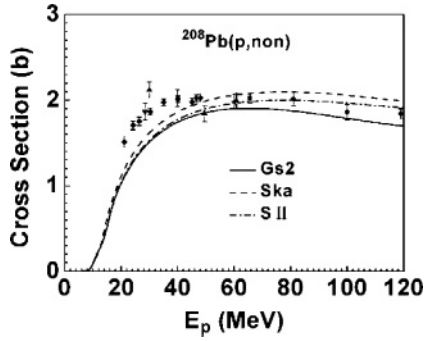

FIG. 20. Calculated proton reaction cross sections compared with experimental data [82,100–104] for $p + {}^{208}$Pb reaction. The theoretical values computed with GS2 are shown as the solid curve, those computed with Ska are shown as the dashed curve, and those computed with SII are shown as the dot-dashed curve.

data [42,74,92], and the calculated result by GS2 is better in fitting the experimental data than those by Ska and SII.

The calculated neutron elastic scattering angular distributions for ^{208}Pb at incident energies from 1.8 to 65.0 MeV are compared with experimental data [54,93–99] in Fig. 19, the theoretical calculated results are in good agreement with experimental data.

The comparison of calculated results of proton reaction cross sections for ^{208}Pb with experimental data [82,100–104] is given in Fig. 20. The shapes of calculated results by GS2, Ska, and SII are similar to the experimental data. The calculated values by SII are in reasonable agreement with the experimental data for the incident energy higher than 50 MeV, where for the lower energies, the magnitudes of calculated results by GS2, Ska, and SII are all smaller than those of experimental data.

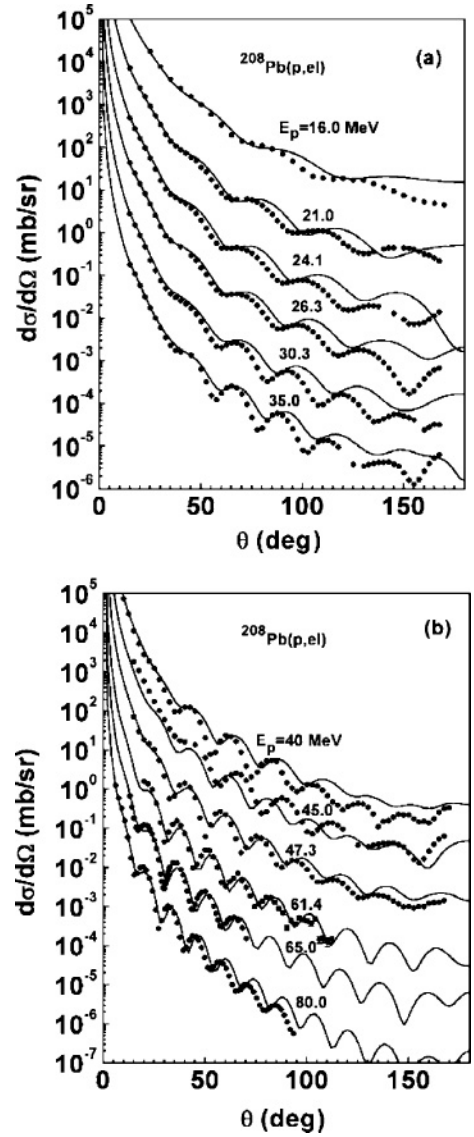

FIG. 21. Calculated elastic scattering angular distributions (solid line) compared with experimental data [68,85,105–107] for $p + {}^{208}$Pb reaction. The results are offset by factors of 10.

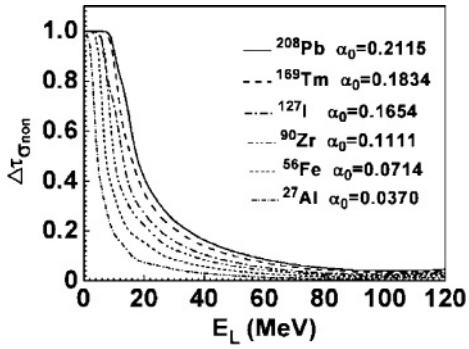

FIG. 22. The calculated isospin effect values for different target nucleus by MOP below 120 MeV.

The calculated proton elastic scattering angular distributions for ^{208}Pb at incident energies from 16.0 to 80.0 MeV are compared with experimental data [68,85,105–107] in Fig. 21. For the energies below 40 MeV, the theoretical calculated results are in good agreement with experimental data for the angles less than 70 degrees, while for the greater angles, the calculated values are inconsistent with the experimental data. For the higher energy, the theoretical calculated results are in reasonable agreement with experimental data.

We define the isospin effect value as

$$\Delta\tau_{\sigma_{\rm non}} = \frac{\sigma_{{\rm non},n} - \sigma_{{\rm non},p}}{\sigma_{{\rm non},n} + \sigma_{{\rm non},p}}. \tag{4.1}$$

The target nuclei with different asymmetric parameter α_0 given by Eq. (3.49) are chosen. They are ^{208}Pb ($\alpha_0 = 0.2115$), ^{169}Tm($\alpha_0 = 0.1834$), ^{127}I($\alpha_0 = 0.1654$), ^{90}Zr ($\alpha_0 = 0.1111$), ^{56}Fe ($\alpha_0 = 0.0714$), and ^{27}Al ($\alpha_0 = 0.0370$). Their neutron and proton nonelastic cross sections are calculated by MOP for incident energies below 120 MeV. The calculated isospin effect values are shown in Fig. 22. For very low energy $\sigma_{{\rm non},p}$ equals zero, then $\Delta\tau_{\sigma_{\rm non}}$ tend to 1. The calculated results show that the isopin effect value decreases as the incident energy increases and increases as the asymmetric parameter α_0 of the target nucleus increases. The isopin effect value above 100 MeV even for ^{208}Pb($\alpha_0 = 0.2115$) is less than 0.05, which means that in the high energy region the isospin effect is very small. These results are reasonable.

V. SUMMARY

In this paper we have presented the progress of our effort on the microscopic theory of the nucleon-nucleus optical potential with Skyrme interactions and its applications. With certain versions of the Skyrme interactions we have obtained the microscopic optical potential for finite nuclei (via the local density approximation) which shows that for certain energy regions the potential depth, shape, relative contributions of the surface and volume parts, as well as the energy dependences are in reasonable agreement with the phenomenological optical potentials and those based on realistic nucleon-nucleon interaction. The calculated results, such as the total and nonelastic cross sections and angular distributions of elastic scattering, are in good agreement with the experimental data and, to a certain extent, comparable with the phenomenological optical potentials. The comparisons among the different versions of Skyrme interactions show that all the real parts (only HF term included) with various Skyrme interactions are close to each other, while the imaginary parts with those differ very much. Considering both the real and imaginary parts as a whole among all kinds of Skyrme interactions the GS2 is the best, and the Ska and Skb are good. We also define the ratio of the difference and summation of the neutron and proton nonelastic cross sections as the isospin effect value. The calculated results show that the isopin effect value decreases as the incident energy increases and increases as the asymmetric parameter $\alpha_0 = (N\text{-}Z)/A$ of the target nucleus increases.

ACKNOWLEDGMENTS

This work is one of National Basic Research Program of China (973 Program), that is Key Technology Research of Accelerator Driven Sub-critical System for Nuclear Waste Transmutation, and supported by the China Ministry of Science and Technology under Contract No. 2007CB209903. The authors thank Dr. B. K. Wilson for discussions and help.

APPENDIX A: INTEGRALS OF THREE MOMENTUM VECTORS FOR ASYMMETRIC NUCLEAR MATTER

The seven integrals in Eq. (3.43) are evaluated in this appendix. The energy ε_τ of a particle or a hole is related to the effective mass m^*_τ as

$$\varepsilon_\tau = \frac{\hbar^2 k^2}{2m_\tau} + V_\tau = \frac{\hbar^2 k^2}{2m^*_\tau} + V^0_\tau, \tag{A1}$$

V^0_τ is a constant. Let

$$\beta_\tau = \frac{\hbar^2}{2m^*_\tau}. \tag{A2}$$

According to the conservation of charge,

$$\varepsilon_\alpha + \varepsilon_\nu - \varepsilon_\lambda - \varepsilon_\mu = \beta_{\tau_\alpha} k^2_\alpha + \beta_{\tau_\nu} k^2_\nu - \beta_{\tau_\alpha} k^2_\lambda - \beta_{\tau_\nu} k^2_\mu. \tag{A3}$$

Thus Eq. (3.43) can be expressed as

$$I_i(\tau_\alpha, \tau_\nu) = \int \mathrm{d}\vec{k}_\nu \mathrm{d}\vec{k}_\lambda \mathrm{d}\vec{k}_\mu f_i(\vec{k}_{\alpha\nu}, \vec{k}_{\lambda\mu}) \delta(\vec{k}_\alpha + \vec{k}_\nu - \vec{k}_\lambda - \vec{k}_\mu) \times \delta\left(\beta_{\tau_\alpha} k^2_\alpha + \beta_{\tau_\nu} k^2_\nu - \beta_{\tau_\alpha} k^2_\lambda - \beta_{\tau_\nu} k^2_\mu\right). \tag{A4}$$

Let

$$\vec{k}_p = \vec{k}_\lambda + \vec{k}_\mu, \quad \vec{q}_p = \tfrac{1}{2}(\vec{k}_\lambda - \vec{k}_\mu). \tag{A5}$$

It is easy to proved that $\mathrm{d}\vec{k}_\lambda \mathrm{d}\vec{k}_\mu = \mathrm{d}\vec{k}_p \mathrm{d}\vec{q}_p$, and it can be seen that

$$\vec{k}_\lambda = \tfrac{1}{2}\vec{k}_p + \vec{q}_p, \quad \vec{k}_\mu = \tfrac{1}{2}\vec{k}_p - \vec{q}_p, \tag{A6}$$

$$\vec{k}_\lambda - \vec{k}_\mu = 2\vec{q}_p,$$

$$k^2_\lambda = \tfrac{1}{4}k^2_p + q^2_p + \vec{k}_p \cdot \vec{q}_p, \tag{A7}$$

$$k^2_\mu = \tfrac{1}{4}k^2_p + q^2_p - \vec{k}_p \cdot \vec{q}_p,$$

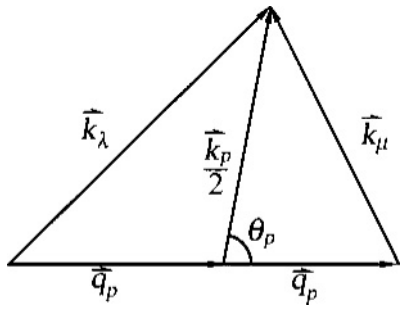

FIG. 23. Momentum composition of two particles.

$$\beta_{\tau_\alpha}k_\lambda^2+\beta_{\tau_\nu}k_\mu^2=\left(\beta_{\tau_\alpha}+\beta_{\tau_\nu}\right)\left(\tfrac{1}{4}k_p^2+q_p^2\right)+\left(\beta_{\tau_\alpha}-\beta_{\tau_\nu}\right)(\vec{k}_p\cdot\vec{q}_p). \tag{A8}$$

According to the conservation of momentum expressed by the first δ function in Eq. (A4), it can be seen that

$$\vec{k}_p=\vec{k}_\alpha+\vec{k}_\nu, \tag{A9}$$

and Eq. (A4) can be reduced to

$$I_i(\tau_\alpha,\tau_\nu)=\int \mathrm{d}\vec{k}_\nu \mathrm{d}\vec{q}_p f_i(\vec{k}_{\alpha\nu},2\vec{q}_p), \times\delta\left(\beta_{\tau_\alpha}k_\alpha^2+\beta_{\tau_\nu}k_\nu^2-\left(\beta_{\tau_\alpha}+\beta_{\tau_\nu}\right)\left(\frac{1}{4}k_p^2+q_p^2\right)-\left(\beta_{\tau_\alpha}-\beta_{\tau_\nu}\right)(\vec{k}_p\cdot\vec{q}_p)\right). \tag{A10}$$

$\vec{k}_p$ is chosen as the pole axis for the integration variable $\vec{q}_p$, the included angle is θ_p (shown as Fig. 23), and $\vec{k}_\alpha$ is chosen as the pole axis for the integration variable $\vec{k}_\nu$, the included angle is θ_ν, and $\mu=\cos\theta_\nu$, so

$$k_p=\sqrt{k_\alpha^2+k_\nu^2+2k_\alpha k_\nu\mu}. \tag{A11}$$

In Eq. (A10), for $i=1,2,3$, $f_i(k_{\alpha\nu},2\vec{q}_p)$ is only dependent on the absolute values of $\vec{k}_{\alpha\nu}$ and $\vec{q}_p$, so $I_i(\tau_\alpha,\tau_\nu)$ can be rewritten as

$$\begin{aligned}I_i(\tau_\alpha,\tau_\nu)&=(2\pi)^2\int k_\nu^2\mathrm{d}k_\nu\int_{-1}^{1}\mathrm{d}\mu \times\int q_p^2\mathrm{d}q_p\int \mathrm{d}\cos\theta_p f_i\left(\vec{k}_{\alpha\nu},2\vec{q}_p\right) \times\delta\left(\beta_{\tau_\alpha}k_\alpha^2+\beta_{\tau_\nu}k_\nu^2-\left(\beta_{\tau_\alpha}+\beta_{\tau_\nu}\right)\left(\frac{1}{4}k_p^2+q_p^2\right)-\left(\beta_{\tau_\alpha}-\beta_{\tau_\nu}\right)k_pq_p\cos\theta_p\right)\\&=\frac{(2\pi)^2}{\beta_{\tau_\alpha}-\beta_{\tau_\nu}}\int k_\nu^2\mathrm{d}k_\nu\int_{-1}^{1}\frac{\mathrm{d}\mu}{k_p}\int q_p\mathrm{d}q_p \times\int \mathrm{d}\cos\theta_p f_i\left(\vec{k}_{\alpha\nu},2\vec{q}_p\right) \times\delta\left(\frac{\beta_{\tau_\alpha}k_\alpha^2+\beta_{\tau_\nu}k_\nu^2-\left(\beta_{\tau_\alpha}+\beta_{\tau_\nu}\right)\left(\frac{1}{4}k_p^2+q_p^2\right)}{\left(\beta_{\tau_\alpha}-\beta_{\tau_\nu}\right)k_pq_p}-\cos\theta_p\right),\quad i=1,2,3.\end{aligned} \tag{A12}$$

k_{τ_α} and k_{τ_ν} are the fermi momentums of nuclons α and ν, respectively. Since $k_\lambda^2\geqslant k_{\tau_\alpha}^2$, $k_\mu^2\geqslant k_{\tau_\nu}^2$, it can be obtained from Eq. (A7)

$$\begin{aligned}&\frac{1}{4}k_p^2+q_p^2+k_pq_p\cos\theta_p\geqslant k_{\tau_\alpha}^2,\\&\frac{1}{4}k_p^2+q_p^2-k_pq_p\cos\theta_p\geqslant k_{\tau_\nu}^2\end{aligned} \tag{A13}$$

$$-\frac{\frac{1}{4}k_p^2+q_p^2-k_{\tau_\alpha}^2}{k_pq_p}\leqslant\cos\theta_p\leqslant\frac{\frac{1}{4}k_p^2+q_p^2-k_{\tau_\nu}^2}{k_pq_p}. \tag{A14}$$

Equation (A14) gives the range of $\cos\theta_p$. According to the upper limit of $\cos\theta_p$ and the δ function in Eq. (A12), it can be obtained that

$$\begin{aligned}&\left(\beta_{\tau_\alpha}-\beta_{\tau_\nu}\right)\left(\frac{1}{4}k_p^2+q_p^2-k_{\tau_\nu}^2\right)\\&\quad\geqslant\beta_{\tau_\alpha}k_\alpha^2+\beta_{\tau_\nu}k_\nu^2-\left(\beta_{\tau_\alpha}+\beta_{\tau_\nu}\right)\left(\frac{1}{4}k_p^2+q_p^2\right),\\&q_p^2\geqslant\frac{H_1+\beta_{\tau_\nu}k_\nu^2-\frac{1}{2}\beta_{\tau_\alpha}k_p^2}{2\beta_{\tau_\alpha}}\equiv Q_1^2,\end{aligned} \tag{A15}$$

where

$$H_1=\beta_{\tau_\alpha}k_\alpha^2+\left(\beta_{\tau_\alpha}-\beta_{\tau_\nu}\right)k_{\tau_\nu}^2. \tag{A16}$$

According to the lower limit of $\cos\theta_p$ and the δ function in Eq. (A12), it can be obtained that

$$\begin{aligned}&-\left(\beta_{\tau_\alpha}-\beta_{\tau_\nu}\right)\left(\frac{1}{4}k_p^2+q_p^2-k_{\tau_\alpha}^2\right)\\&\quad\leqslant\beta_{\tau_\alpha}k_\alpha^2+\beta_{\tau_\nu}k_\nu^2-\left(\beta_{\tau_\alpha}+\beta_{\tau_\nu}\right)\left(\frac{1}{4}k_p^2+q_p^2\right)\\&q_p^2\leqslant\frac{H_2+\beta_{\tau_\nu}k_\nu^2-\frac{1}{2}\beta_{\tau_\nu}k_p^2}{2\beta_{\tau_\nu}}\equiv Q_2^2,\end{aligned} \tag{A17}$$

where

$$H_2=\beta_{\tau_\alpha}k_\alpha^2-\left(\beta_{\tau_\alpha}-\beta_{\tau_\nu}\right)k_{\tau_\alpha}^2. \tag{A18}$$

Then Eq. (A12) can be reduced to

$$I_i(\tau_\alpha,\tau_\nu)=\frac{(2\pi)^2}{\beta_{\tau_\alpha}-\beta_{\tau_\nu}}\int k_\nu^2\mathrm{d}k_\nu\int_{-1}^{1}\frac{\mathrm{d}\mu}{k_p} \times\int_{Q_1}^{Q_2}q_pf_i(\vec{k}_{\alpha\nu},2\vec{q}_p)\mathrm{d}q_p,\quad i=1,2,3. \tag{A19}$$

Since $f_1=1$, $I_1(\tau_\alpha,\tau_\nu)$ can be expressed as

$$I_1(\tau_\alpha,\tau_\nu)=\frac{(2\pi)^2}{2}\int k_\nu^2\mathrm{d}k_\nu\int_{-1}^{1}\frac{\mathrm{d}\mu}{k_p}\frac{Q_2^2-Q_1^2}{\beta_{\tau_\alpha}-\beta_{\tau_\nu}}. \tag{A20}$$

It can be obtained form Eqs. (A15)–(A18) that

$$Q_2^2-Q_1^2=\frac{\beta_{\tau_\alpha}-\beta_{\tau_\nu}}{2\beta_{\tau_\alpha}}\left(k_\nu^2-B_0\right), \tag{A21}$$

where

$$B_0=\frac{1}{\beta_{\tau_\nu}}\left[\beta_{\tau_\nu}k_{\tau_\nu}^2-\beta_{\tau_\alpha}\left(k_\alpha^2-k_{\tau_\alpha}^2\right)\right]. \tag{A22}$$

Then it is easy to get

$$I_1(\tau_\alpha, \tau_v) = \frac{\pi^2}{\beta_{\tau_\alpha}} \int \left(k_v^2 - B_0\right) k_v^2 \mathrm{d}k_v \int_{-1}^{1} \frac{\mathrm{d}\mu}{k_p} \tag{A23}$$

and then

$$I_1(\tau_\alpha, \tau_v) = \frac{2\pi^2}{\beta_{\tau_\alpha} k_\alpha} \int \left(k_v^2 - B_0\right) k_v^2 \mathrm{d}k_v. \tag{A24}$$

According to the δ function in Eq. (A4),

$$\beta_{\tau_\alpha} k_\alpha^2 + \beta_{\tau_v} k_v^2 = \beta_{\tau_\alpha} k_\lambda^2 + \beta_{\tau_v} k_\mu^2 \geqslant \beta_{\tau_\alpha} k_{\tau_\alpha}^2 + \beta_{\tau_v} k_{\tau_v}^2,$$

k_v must satisfy

$$k_v^2 \geqslant B_0 \tag{A25}$$

so the range of k_v can be

$$k_{\tau_v} \geqslant k_v \geqslant \begin{cases} 0 & B_0 \leqslant 0 \\ \sqrt{B_0} & B_0 > 0 \end{cases}. \tag{A26}$$

Then the integral (A24) can be obtained:

$$I_1(\tau_\alpha, \tau_v) = \frac{2\pi^2}{15\beta_{\tau_\alpha} k_\alpha} \left[\left(3k_{\tau_v}^2 - 5B_0\right) k_{\tau_v}^3 + 2B_0^{5/2} \Theta(B_0)\right], \tag{A27}$$

where

$$\Theta(B_0) = \begin{cases} 1 & B_0 \geqslant 0 \\ 0 & B_0 < 0 \end{cases}. \tag{A28}$$

It can be obtained similarly that

$$\begin{aligned} I_2(\tau_\alpha, \tau_v) = {} & \frac{\pi^2}{105\beta_{\tau_\alpha} k_\alpha} \frac{1}{\beta_{\tau_\alpha} \beta_{\tau_v}} \left\{\left[15B_2 k_{\tau_v}^4 + 21(B_1 - B_0 B_2) k_{\tau_v}^2 \right.\right. \\ & \left.\left. - 35B_0 B_1\right] k_{\tau_v}^3 + 2(7B_1 + 3B_0 B_2) B_0^{5/2} \Theta(B_0)\right\}, \end{aligned} \tag{A29}$$

$$\begin{aligned} I_3(\tau_\alpha, \tau_v) = {} & \frac{2\pi^2}{945\beta_{\tau_\alpha} k_\alpha} \frac{1}{\beta_{\tau_\alpha}^2 \beta_{\tau_v}^2} \left\{\left[35B_5 k_{\tau_v}^6 + 45(B_4 - B_0 B_5) k_{\tau_v}^4 \right.\right. \\ & + 63(B_3 - B_0 B_4) k_{\tau_v}^2 - 105 B_0 B_3\left.\right] k_{\tau_v}^3 \\ & \left.\left. + 2\left(21B_3 + 9B_0 B_4 + 5B_0^2 B_5\right) B_0^{5/2} \Theta(B_0)\right\}, \end{aligned} \tag{A30}$$

where

$$\begin{aligned} B_1 &= \beta_{\tau_\alpha} H_2 + \beta_{\tau_v} H_1, \quad B_2 = \left(\tfrac{7}{3}\beta_{\tau_\alpha} + \beta_{\tau_v}\right)\beta_{\tau_v}, \\ B_3 &= B_1^2 - \beta_{\tau_\alpha} \beta_{\tau_v} H_1 H_2, \\ B_4 &= \left[2\left(\beta_{\tau_\alpha}^2 H_2 + \beta_{\tau_v}^2 H_1\right) + \beta_{\tau_\alpha} \beta_{\tau_v} (H_1 + H_2)\right. \\ &\quad \left. + 2\beta_{\tau_\alpha} B_1 + 4\beta_{\tau_\alpha}^2 \beta_{\tau_v} k_\alpha^2\right]\beta_{\tau_v}, \\ B_5 &= \left(\tfrac{23}{5}\beta_{\tau_\alpha}^2 + 3\beta_{\tau_\alpha}\beta_{\tau_v} + \beta_{\tau_v}^2\right)\beta_{\tau_v}^2. \end{aligned} \tag{A31}$$

According to Eqs. (3.44) and (A6), f_4 can be expressed as

$$f_4 = 2\vec{k}_{\alpha v} \cdot \vec{q}_p. \tag{A32}$$

Let β be the include angle between $\vec{k}_{\alpha v}$ and $\vec{q}_p$, $(\theta_0, \varphi_0 = 0)$ be the solid angle between $\vec{k}_{\alpha v}$ and $\vec{k}_p$, and (θ_p, φ_p) be the solid angle between $\vec{q}_p$ and $\vec{k}_p$, then

$$\cos\beta = \cos\theta_0 \cos\theta_p + \sin\theta_0 \sin\theta_p \cos\varphi_p. \tag{A33}$$

Then $I_4(\tau_\alpha, \tau_v)$ can be expressed as

$$\begin{aligned} I_4(\tau_\alpha, \tau_v) = {} & 2\int k_{\alpha v} \mathrm{d}\vec{k}_v \int q_p \cos\beta q_p^2 \mathrm{d}q_p \mathrm{d}\cos\theta_p \mathrm{d}\varphi_p \\ & \times \delta\left(\beta_{\tau_\alpha} k_\alpha^2 + \beta_{\tau_v} k_v^2 - \left(\beta_{\tau_\alpha} + \beta_{\tau_v}\right)\left(\frac{1}{4}k_p^2 + q_p^2\right)\right. \\ & \left. - \left(\beta_{\tau_\alpha} - \beta_{\tau_v}\right) k_p q_p \cos\theta_p\right) \\ = {} & \frac{2}{\beta_{\tau_\alpha} - \beta_{\tau_v}} \int \frac{k_{\alpha v}}{k_p} \mathrm{d}\vec{k}_v \\ & \times \int q_p^2 \mathrm{d}q_p \int \mathrm{d}\cos\theta_p \int \cos\beta \mathrm{d}\varphi_p \\ & \times \delta\left(\frac{\beta_{\tau_\alpha} k_\alpha^2 + \beta_{\tau_v} k_v^2 - \left(\beta_{\tau_\alpha} + \beta_{\tau_v}\right)\left(\frac{1}{4}k_p^2 + q_p^2\right)}{\left(\beta_{\tau_\alpha} - \beta_{\tau_v}\right) k_p q_p}\right. \\ & \left. - \cos\theta_p\right). \end{aligned} \tag{A34}$$

Since

$$\cos\theta_0 = \frac{\vec{k}_{\alpha v} \cdot \vec{k}_p}{k_{\alpha v} k_p} = \frac{k_\alpha^2 - k_v^2}{k_{\alpha v} k_p} \tag{A35}$$

from Eq. (A33) it can be obtained that

$$\int_0^{2\pi} \cos\beta \mathrm{d}\varphi_p = 2\pi \cos\theta_0 \cos\theta_p = 2\pi \frac{k_\alpha^2 - k_v^2}{k_{\alpha v} k_p} \cos\theta_p. \tag{A36}$$

Then $I_4(\tau_\alpha, \tau_v)$ can be expressed as

$$I_4(\tau_\alpha, \tau_v) = \frac{4\pi}{\left(\beta_{\tau_\alpha} - \beta_{\tau_v}\right)^2} \int \left(k_\alpha^2 - k_v^2\right) \frac{1}{k_p^3} X_4 \mathrm{d}\vec{k}_v, \tag{A37}$$

where

$$X_4 = \int_{Q_1}^{Q_2} q_p \left[\beta_{\tau_\alpha} k_\alpha^2 + \beta_{\tau_v} k_v^2 - \left(\beta_{\tau_\alpha} + \beta_{\tau_v}\right)\left(\frac{1}{4}k_P^2 + q_p^2\right)\right] \mathrm{d}q_p. \tag{A38}$$

Q_1 and Q_2 are given in Eqs. (A15) and (A17). The X_4 can be expressed as

$$X_4 = \frac{1}{8\beta_{\tau_\alpha}} \left(\beta_{\tau_\alpha} - \beta_{\tau_v}\right)^2 \left(k_v^2 - B_0\right)\left(B_6 + B_7 k_v^2\right), \tag{A39}$$

where

$$\begin{aligned} B_6 &= \left(k_{\tau_\alpha}^2 - k_{\tau_v}^2\right) + \frac{1}{2\beta_{\tau_\alpha}} \left(\beta_{\tau_\alpha} - \beta_{\tau_v}\right) B_0, \\ B_7 &= -\frac{1}{2\beta_{\tau_\alpha}} \left(\beta_{\tau_\alpha} - \beta_{\tau_v}\right). \end{aligned} \tag{A40}$$

Then the integral of $I_4(\tau_\alpha, \tau_v)$ can be expressed as

$$I_4(\tau_\alpha, \tau_v) = \frac{2\pi^2}{\beta_{\tau_\alpha} k_\alpha} \int k_v^2 \left(k_v^2 - B_0\right)\left(B_6 + B_7 k_v^2\right) \mathrm{d}k_v. \tag{A41}$$

And according to Eq. (A26), it can be obtained that

$$I_4(\tau_\alpha,\tau_v) = \frac{2\pi^2}{105\beta_{\tau_\alpha}k_\alpha}\{[15B_7k_{\tau_v}^4 + 21(B_6 - B_0B_7)k_{\tau_v}^2 - 35B_0B_6]k_{\tau_v}^3 + 2(7B_6 + 3B_0B_7)B_0^{5/2}\Theta(B_0)\}. \quad \text{(A42)}$$

It can be obtained similarly that

$$\begin{aligned} I_5(\tau_\alpha,\tau_v) &= \frac{\pi^2}{315\beta_{\tau_\alpha}k_\alpha}\{[35B_{10}k_{\tau_v}^6 + 45(B_9 - B_0B_{10})k_{\tau_v}^4 \\ &\quad + 63(B_8 - B_0B_9)k_{\tau_v}^2 - 105B_0B_8]k_{\tau_v}^3 \\ &\quad + 2(21B_8 + 9B_0B_9 + 5B_0^2B_{10})B_0^{5/2}\Theta(B_0)\}, \\ I_6(\tau_\alpha,\tau_v) &= \frac{2\pi^2}{945\beta_{\tau_\alpha}k_\alpha}\{[35B_{13}k_{\tau_v}^6 + 45(B_{12} - B_0B_{13})k_{\tau_v}^4 \\ &\quad + 63(B_{11} - B_0B_{12})k_{\tau_v}^2 - 105B_0B_{11}]k_{\tau_v}^3 \\ &\quad + 2(21B_{11} + 9B_0B_{12} + 5B_0^2B_{13})B_0^{5/2}\Theta(B_0)\}, \\ I_7(\tau_\alpha,\tau_v) &= I_3'(\tau_\alpha,\tau_v) - I_6(\tau_\alpha,\tau_v), \end{aligned} \quad \text{(A43)}$$

where

$$\begin{aligned} B_8 &= F_1B_6 - F_0B_0^2, \quad B_9 = F_2B_6 + F_1B_7 + 2F_0B_0, \\ B_{10} &= F_2B_7 - F_0, \quad F_0 = \frac{1}{6\beta_{\tau_\alpha}^2}(\beta_{\tau_\alpha}^2 - \beta_{\tau_v}^2), \\ F_1 &= \frac{1}{\beta_{\tau_\alpha}\beta_{\tau_v}}[(\beta_{\tau_\alpha} + \beta_{\tau_v})\beta_{\tau_\alpha}k_\alpha^2 \\ &\quad - (\beta_{\tau_\alpha} - \beta_{\tau_v})(\beta_{\tau_\alpha}k_{\tau_\alpha}^2 - \beta_{\tau_v}k_{\tau_v}^2)], \\ F_2 &= 4 + S, \quad S = \frac{1}{\beta_{\tau_\alpha}}(\beta_{\tau_\alpha} + \beta_{\tau_v}), \\ B_{11} &= 3B_6^2 + \frac{1}{4}S^2B_0^2, \\ B_{12} &= 4F_1 - 4k_\alpha^2 + 6B_6B_7 - \frac{1}{2}S^2B_0, \\ B_{13} &= 3B_7^2 + 4S + \frac{1}{4}S^2 + \frac{4}{5}, \end{aligned} \quad \text{(A44)}$$

$$\begin{aligned} I_3'(\tau_\alpha,\tau_v) &= \frac{2\pi^2}{945\beta_{\tau_\alpha}k_\alpha}\{[35B_{16}k_{\tau_v}^6 + 45(B_{15} - B_0B_{16})k_{\tau_v}^4 \\ &\quad + 63(B_{14} - B_0B_{15})k_{\tau_v}^2 - 105B_0B_{14}]k_{\tau_v}^3 \\ &\quad + 2(21B_{14} + 9B_0B_{15} + 5B_0^2B_{16})B_0^{5/2}\Theta(B_0)\}, \\ B_{14} &= 3(F_1 - k_\alpha^2)k_\alpha^2, \quad B_{15} = 5F_1 + (3S - 2)k_\alpha^2, \\ B_{16} &= 5S - \frac{7}{5}. \end{aligned}$$

APPENDIX B: INTEGRALS OF FIVE MOMENTUM VECTORS FOR ASYMMETRIC NUCLEAR MATTER

The integral

$$\begin{aligned} I_B(\tau_\alpha,\tau_v,\tau_\zeta) \equiv I_B(\tau_\alpha\tau_v\tau_\zeta\tau_\alpha\tau_v\tau_\zeta) &= \int \mathrm{d}\vec{k}_v\mathrm{d}\vec{k}_\zeta\mathrm{d}\vec{k}_\lambda\mathrm{d}\vec{k}_\mu\mathrm{d}\vec{k}_\xi \\ &\quad \times \delta(\vec{k}_\alpha + \vec{k}_v + \vec{k}_\zeta - \vec{k}_\lambda - \vec{k}_\mu - \vec{k}_\xi) \\ &\quad \times \delta(\varepsilon_\alpha + \varepsilon_v + \varepsilon_\zeta - \varepsilon_\lambda - \varepsilon_\mu - \varepsilon_\xi) \end{aligned} \quad \text{(B1)}$$

expressed in Eq. (3.45) is reduced in this appendix.

According to Eqs. (A1) and (A2) and the conservation of charge it can be seen that

$$\begin{aligned} &\varepsilon_\alpha + \varepsilon_v + \varepsilon_\zeta - \varepsilon_\lambda - \varepsilon_\mu - \varepsilon_\xi \\ &\quad = \beta_{\tau_\alpha}k_\alpha^2 + \beta_{\tau_v}k_v^2 + \beta_{\tau_\zeta}k_\zeta^2 - \beta_{\tau_\alpha}k_\lambda^2 - \beta_{\tau_v}k_\mu^2 - \beta_{\tau_\zeta}k_\xi^2. \end{aligned} \quad \text{(B2)}$$

Let

$$\begin{aligned} \vec{k}_p &= \vec{k}_\mu + \vec{k}_\xi, \quad \vec{q}_p = \tfrac{1}{2}(\vec{k}_\mu - \vec{k}_\xi), \\ \vec{k}_h &= \vec{k}_v + \vec{k}_\zeta, \quad \vec{q}_h = \tfrac{1}{2}(\vec{k}_v - \vec{k}_\zeta). \end{aligned} \quad \text{(B3)}$$

It is easy to proved that $\mathrm{d}\vec{k}_p\mathrm{d}\vec{q}_p = \mathrm{d}\vec{k}_\mu\mathrm{d}\vec{k}_\xi, \mathrm{d}\vec{k}_h\mathrm{d}\vec{q}_h = \mathrm{d}\vec{k}_v\mathrm{d}\vec{k}_\zeta$, and it can be seen that

$$\vec{k}_\mu = \tfrac{1}{2}\vec{k}_p + \vec{q}_p, \quad \vec{k}_\xi = \tfrac{1}{2}\vec{k}_p - \vec{q}_p, \quad \text{(B4)}$$

$$\vec{k}_v = \tfrac{1}{2}\vec{k}_h + \vec{q}_h, \quad \vec{k}_\zeta = \tfrac{1}{2}\vec{k}_h - \vec{q}_h, \quad \text{(B5)}$$

$$k_\mu^2 + k_\xi^2 = \tfrac{1}{2}k_p^2 + 2q_p^2, \quad k_v^2 + k_\zeta^2 = \tfrac{1}{2}k_h^2 + 2q_h^2, \quad \text{(B6)}$$

$$\beta_{\tau_v}k_\mu^2 + \beta_{\tau_\zeta}k_\xi^2 = \beta_+(\tfrac{1}{4}k_p^2 + q_p^2) + \beta_-(\vec{k}_p\cdot\vec{q}_p), \quad \text{(B7)}$$

$$\beta_{\tau_v}k_v^2 + \beta_{\tau_\zeta}k_\zeta^2 = \beta_+(\tfrac{1}{4}k_h^2 + q_h^2) + \beta_-(\vec{k}_h\cdot\vec{q}_h), \quad \text{(B8)}$$

where

$$\beta_\pm = \beta_{\tau_v} \pm \beta_{\tau_\zeta}. \quad \text{(B9)}$$

Using the conservation of momentum expressed by the first δ function in Eq. (B1), the integral of $I_B(\tau_\alpha,\tau_v,\tau_\zeta)$ can be reduced to

$$\begin{aligned} I_B(\tau_\alpha,\tau_v,\tau_\zeta) = \int \mathrm{d}\vec{k}_h\mathrm{d}\vec{q}_h\mathrm{d}\vec{k}_p\mathrm{d}\vec{q}_p\delta(&\beta_{\tau_\alpha}k_\alpha^2 + \beta_+(\tfrac{1}{4}k_h^2 + q_h^2) \\ &+ \beta_-k_hq_h\cos\alpha_h - \beta_+(\tfrac{1}{4}k_p^2 + q_p^2) \\ &- \beta_-k_pq_p\cos\alpha_p - \beta_{\tau_\alpha}(\vec{k}_\alpha + \vec{k}_h - \vec{k}_p)^2), \end{aligned} \quad \text{(B10)}$$

where α_h is the included angle of $\vec{k}_h$ and $\vec{q}_h$, α_p is the included angle of $\vec{k}_p$ and $\vec{q}_p$.

Since $k_\mu \geqslant k_{\tau_v}$ and $k_\xi \geqslant k_{\tau_\zeta}$, from Eq. (B4) it can be obtained that

$$\left(\frac{1}{2}\vec{k}_p + \vec{q}_p\right)^2 = \frac{1}{4}k_p^2 + q_p^2 + k_pq_p\cos\alpha_p \geqslant k_{\tau_v}^2,$$

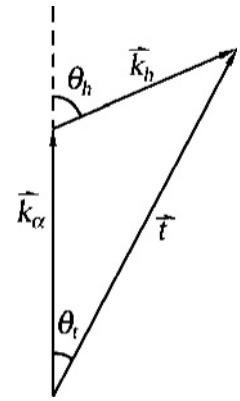

FIG. 24. The kinematic transformation for hole.

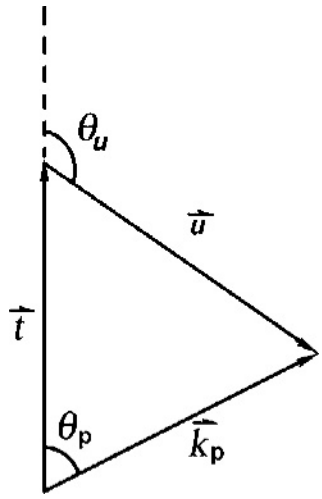

FIG. 25. The kinematic transformation for particle.

$$\left(\frac{1}{2}\vec{k}_p - \vec{q}_p\right)^2 = \frac{1}{4}k_p^2 + q_p^2 - k_p q_p \cos\alpha_p \geqslant k_{\tau_\zeta}^2,$$
$$-\frac{\frac{1}{4}k_p^2 + q_p^2 - k_{\tau_v}^2}{k_p q_p} \leqslant \cos\alpha_p \leqslant \frac{\frac{1}{4}k_p^2 + q_p^2 - k_{\tau_\zeta}^2}{k_p q_p}. \quad \text{(B11)}$$

And since $k_v \leqslant k_{\tau_v}$ and $k_\zeta \leqslant k_{\tau_\zeta}$, from Eq. (B5) it can be obtained that

$$\left(\frac{1}{2}\vec{k}_h + \vec{q}_h\right)^2 = \frac{1}{4}k_h^2 + q_h^2 + k_h q_h \cos\alpha_h \leqslant k_{\tau_v}^2,$$
$$\left(\frac{1}{2}\vec{k}_h - \vec{q}_h\right)^2 = \frac{1}{4}k_h^2 + q_h^2 - k_h q_h \cos\alpha_h \leqslant k_{\tau_\zeta}^2,$$
$$-\frac{k_{\tau_\zeta}^2 - \frac{1}{4}k_h^2 - q_h^2}{k_h q_h} \leqslant \cos\alpha_h \leqslant \frac{k_{\tau_v}^2 - \frac{1}{4}k_h^2 - q_h^2}{k_h q_h}. \quad \text{(B12)}$$

In the case of $\tau_\zeta = \tau_v$ the integral of $I_B(\tau_\alpha, \tau_v, \tau_v)$ in (B10) can be rewritten as

$$I_B(\tau_\alpha, \tau_v, \tau_v) = \int \mathrm{d}\vec{k}_h \mathrm{d}\vec{q}_h \mathrm{d}\vec{k}_p \mathrm{d}\vec{q}_p \delta\left(\beta_{\tau_\alpha} k_\alpha^2 + 2\beta_{\tau_\alpha}\left(\frac{1}{4}k_h^2 + q_h^2\right) - 2\beta_{\tau_v}\left(\frac{1}{4}k_p^2 + q_p^2\right) - \beta_{\tau_\alpha}(\vec{k}_\alpha + \vec{k}_h - \vec{k}_p)^2\right). \quad \text{(B13)}$$

As the δ function in Eq. (B13) is not dependent on $\cos\alpha_p$ and $\cos\alpha_h$, we have

$$\int \mathrm{d}\vec{q}_p = 2\pi \int q_p^2 \mathrm{d}q_p \int \mathrm{d}\cos\alpha_p \equiv 4\pi \int q_p^2 f_p(k_p, q_p)\mathrm{d}q_p, \quad \text{(B14)}$$

where

$$f_p(k_p, q_p) = \frac{1}{2}\int \mathrm{d}\cos\alpha_p. \quad \text{(B15)}$$

According to Eqs. (B11) and (B15) it can be obtained that

$$f_p(k_p, q_p) = \begin{cases} 0 & \frac{1}{4}k_p^2 + q_p^2 \leqslant k_{\tau_v}^2 \\ 1 & \left|\frac{1}{2}k_p - q_p\right| \geqslant k_{\tau_v} \\ \frac{\frac{1}{4}k_p^2 + q_p^2 - k_{\tau_v}^2}{k_p q_p} & \text{in other case} \end{cases}. \quad \text{(B16)}$$

Similarly

$$\int \mathrm{d}\vec{q}_h = 2\pi \int q_h^2 \mathrm{d}q_h \int \mathrm{d}\cos\alpha_h \equiv 4\pi \int q_h^2 f_h(k_h, q_h)\mathrm{d}q_h, \quad \text{(B17)}$$

where

$$f_h(k_h, q_h) = \frac{1}{2}\int \mathrm{d}\cos\alpha_h. \quad \text{(B18)}$$

According to Eqs. (B12) and (B18) it can be obtained that

$$f_h(k_h, q_h) = \begin{cases} 0 & \frac{1}{4}k_h^2 + q_h^2 \geqslant k_{\tau_v}^2 \\ 1 & \frac{1}{2}k_h + q_h \leqslant k_{\tau_v} \\ \frac{k_{\tau_v}^2 - \frac{1}{4}k_h^2 - q_h^2}{k_h q_h} & \text{in other case} \end{cases}. \quad \text{(B19)}$$

$(\vec{k}_\alpha + \vec{k}_h)$ is chosen as the pole axis for the integration variable $\vec{k}_p$, the included angle is θ_p, and $\vec{k}_\alpha$ is chosen as the pole axis for the integration variable $\vec{k}_h$, the included angle is θ_h, and then $I_B(\tau_\alpha, \tau_v, \tau_v)$ can be expressed as

$$I_B(\tau_\alpha, \tau_v, \tau_v) = 64\pi^4 \int q_h^2 \mathrm{d}q_h \int k_h^2 f_h(k_h, q_h)\mathrm{d}k_h \int \mathrm{d}\cos\theta_h \times \int q_p^2 \mathrm{d}q_p \int k_p^2 f_p(k_p, q_p)\mathrm{d}k_p \int \mathrm{d}\cos\theta_p \times \delta\left(\beta_{\tau_\alpha} k_\alpha^2 + 2\beta_{\tau_\alpha}\left(\frac{1}{4}k_h^2 + q_h^2\right) - 2\beta_{\tau_v}\left(\frac{1}{4}k_p^2 + q_p^2\right) - \beta_{\tau_\alpha}(\vec{k}_\alpha + \vec{k}_h - \vec{k}_p)^2\right). \quad \text{(B20)}$$

Let

$$\vec{t} = \vec{k}_\alpha + \vec{k}_h, \quad s_h = \sqrt{\frac{k_h^2}{4} + q_h^2} \quad \text{(B21)}$$

and θ_t be the included angle between $\vec{k}_\alpha$ and $\vec{t}$ (shown as Fig. 24). It can be gotten from Eq. (B21) that

$$k_h = \sqrt{k_\alpha^2 + t^2 - 2k_\alpha t\cos\theta_t}, \quad \text{(B22)}$$
$$\cos\theta_h = \frac{t\cos\theta_t - k_\alpha}{\sqrt{k_\alpha^2 + t^2 - 2k_\alpha t\cos\theta_t}}, \quad \text{(B23)}$$
$$q_h = \sqrt{s_h^2 - \frac{1}{4}\left(k_\alpha^2 + t^2 - 2k_\alpha t\cos\theta_t\right)}, \quad \text{(B24)}$$

and the corresponding Jacobian is

$$J_h = \frac{\partial(k_h, \cos\theta_h, q_h)}{\partial(t, \cos\theta_t, s_h)} = \frac{t^2 s_h}{k_h^2 q_h}. \tag{B25}$$

Let

$$\vec{u} = \vec{k}_p - \vec{t}, \quad s_p = \sqrt{\frac{k_p^2}{4} + q_p^2} \tag{B26}$$

and θ_u be the included angle between $\vec{u}$ and $\vec{t}$ (shown as Fig. 25). It can be gotten from Eq. (B26) that

$$k_p = \sqrt{t^2 + u^2 + 2tu\cos\theta_u}, \tag{B27}$$

$$\cos\theta_p = \frac{u\cos\theta_u + t}{\sqrt{t^2 + u^2 + 2tu\cos\theta_u}}, \tag{B28}$$

$$q_p = \sqrt{s_p^2 - \frac{1}{4}(t^2 + u^2 + 2tu\cos\theta_u)}, \tag{B29}$$

and the corresponding Jacobian is

$$J_p = \frac{\partial(k_p, \cos\theta_p, q_p)}{\partial(t, \cos\theta_u, s_p)} = \frac{u^2 s_p}{k_p^2 q_p}. \tag{B30}$$

According to Eq. (B19), it is required that $s_h \leqslant k_{\tau_v}$, and let

$$f_1 = \begin{cases} q_h & \frac{1}{2}k_h + q_h \leqslant k_{\tau_v} \\ \frac{1}{k_h}\left(k_{\tau_v}^2 - s_h^2\right) & \frac{1}{2}k_h + q_h > k_{\tau_v} \end{cases}. \tag{B31}$$

According to Eq. (B16), it is required that $s_p > k_{\tau_v}$, and let

$$f_2 = \begin{cases} q_p & q_p > \frac{k_p}{2} + k_{\tau_v} \\ \frac{1}{k_p}\left(s_p^2 - k_{\tau_v}^2\right) & \frac{k_p}{2} - k_{\tau_v} \leqslant q_p \leqslant \frac{k_p}{2} + k_{\tau_v} \\ q_p & q_p < \frac{k_p}{2} - k_{\tau_v} \end{cases}. \tag{B32}$$

It is easy to prove that

$$\vec{u} = -\vec{k}_\lambda. \tag{B33}$$

So $u > k_{\tau_\alpha}$. Using Eqs. (B21), (B25), (B26), (B30), (B31), and (B32), Eq. (B20) can be expressed as

$$\begin{aligned} I_B(\tau_\alpha, \tau_v, \tau_v) = 64\pi^4 &\int^{k_{\tau_v}} s_h \mathrm{d}s_h \int t^2 \mathrm{d}t \int f_1 \mathrm{d}\cos\theta_t \\ &\times \int_{k_{\tau_v}} s_p \mathrm{d}s_p \int_{k_{\tau_\alpha}} u^2 \mathrm{d}u \int f_2 \mathrm{d}\cos\theta_u \\ &\times \delta\left(\beta_{\tau_\alpha} k_\alpha^2 + 2\beta_{\tau_v} s_h^2 - 2\beta_{\tau_v} s_p^2 - \beta_{\tau_\alpha} u^2\right). \end{aligned} \tag{B34}$$

Let

$$z = 2k_\alpha t\cos\theta_t, \quad t\,\mathrm{d}\cos\theta_t = \frac{\mathrm{d}z}{2k_\alpha}, \tag{B35}$$

$$w = 2tu\cos\theta_u, \quad tu\,\mathrm{d}\cos\theta_u = \frac{\mathrm{d}w}{2}. \tag{B36}$$

Since

$$\int s_p \mathrm{d}s_p = \frac{1}{4\beta_{\tau_v}} \int \mathrm{d}\left(2\beta_{\tau_v} s_p^2\right), \tag{B37}$$

Eq. (B34) can be expressed as

$$\begin{aligned} I_B(\tau_\alpha, \tau_v, \tau_v) = \frac{4\pi^4}{\beta_{\tau_v} k_\alpha} &\int^{k_{\tau_v}} s_h \mathrm{d}s_h \int \mathrm{d}t \\ &\times \int f_1 \mathrm{d}z \int_{k_{\tau_\alpha}} u\mathrm{d}u \int f_2 \mathrm{d}w \end{aligned} \tag{B38}$$

and s_p can be expressed as

$$s_p = \left[\frac{\beta_{\tau_\alpha}}{2\beta_{\tau_v}}\left(k_\alpha^2 - u^2\right) + s_h^2\right]^{1/2}. \tag{B39}$$

It is also easy to get that

$$k_h = \sqrt{k_\alpha^2 + t^2 - z}, \tag{B40}$$

$$q_h = \sqrt{s_h^2 - \frac{1}{4}\left(k_\alpha^2 + t^2 - z\right)}, \tag{B41}$$

$$k_p = \sqrt{t^2 + u^2 + w}, \tag{B42}$$

$$q_p = \sqrt{s_p^2 - \frac{1}{4}(t^2 + u^2 + w)}. \tag{B43}$$

Thus the variables k_h, q_h, k_p, q_p, and s_p in Eqs. (B31) and (B32) are given in Eqs. (B39)–(B43).

The range of each integral variable in Eq. (B38) is studied in the following. According to Eqs. (B36) and (B43) w need to satisfy

$$-2tu \leqslant w \leqslant 2tu \tag{B44}$$

and

$$w \leqslant 4s_p^2 - t^2 - u^2. \tag{B45}$$

According to Eqs. (B39) and (B45) it can be obtained that

$$w \leqslant \frac{2\beta_{\tau_\alpha}}{\beta_{\tau_v}} k_\alpha^2 + 4s_h^2 - t^2 - \frac{2\beta_{\tau_\alpha} + \beta_{\tau_v}}{\beta_{\tau_v}} u^2. \tag{B46}$$

From Eqs. (B44) and (B46) one can see that the upper limit of w should be given by Eq. (B46) as u is very large and by Eq. (B44) as u is very little. The connection point between them is the following solution of u when the above two upper limits are equal:

$$\begin{aligned} v = \frac{\beta_{\tau_v}}{2\beta_{\tau_\alpha} + \beta_{\tau_v}} &\left\{-t + \left[t^2 + \frac{2\beta_{\tau_\alpha} + \beta_{\tau_v}}{\beta_{\tau_v}}\right.\right. \\ &\left.\left. \times \left(\frac{2\beta_{\tau_\alpha}}{\beta_{\tau_v}} k_\alpha^2 + 4s_h^2 - t^2\right)\right]^{1/2}\right\}. \end{aligned} \tag{B47}$$

Then the upper limit of w can be obtained

$$N = \begin{cases} \frac{2\beta_{\tau_\alpha}}{\beta_{\tau_v}} k_\alpha^2 + 4s_h^2 - t^2 - \frac{2\beta_{\tau_\alpha} + \beta_{\tau_v}}{\beta_{\tau_v}} u^2 & u > v \\ 2tu & u \leqslant v \end{cases} \tag{B48}$$

and the lower limit of w is $-2tu$.

According to Eq. (B33),

$$u^2 \geqslant k_{\tau_\alpha}^2 \tag{B49}$$

and from Eqs. (B26) and (B3) it can be obtained that

$$s_p^2 \geqslant k_{\tau_v}^2. \tag{B50}$$

Then according to Eq. (B39)

$$u^2 \leqslant k_\alpha^2 - \frac{2\beta_{\tau_v}}{\beta_{\tau_\alpha}}\left(k_{\tau_v}^2 - s_h^2\right) \equiv B_0^2. \tag{B51}$$

From Eqs. (B44) and (B45) it can be obtained that

$$4s_p^2 - t^2 - u^2 \geqslant -2tu. \tag{B52}$$

Then according to Eq. (B39) one obtains

$$\frac{2\beta_{\tau_\alpha} + \beta_{\tau_v}}{\beta_{\tau_v}}u^2 - 2tu - \frac{2\beta_{\tau_\alpha}}{\beta_{\tau_v}}k_\alpha^2 - 4s_h^2 + t^2 \leqslant 0. \tag{B53}$$

When Eq. (B53) is an equality the two solutions of u are

$$B_\pm = \frac{\beta_{\tau_v}}{2\beta_{\tau_\alpha} + \beta_{\tau_v}}\left\{t \pm \left[t^2 + \frac{2\beta_{\tau_\alpha} + \beta_{\tau_v}}{\beta_{\tau_v}} \times \left(\frac{2\beta_{\tau_\alpha}}{\beta_{\tau_v}}k_\alpha^2 + 4s_h^2 - t^2\right)\right]^{1/2}\right\}. \tag{B54}$$

Therefore $B_- \leqslant u \leqslant B_+$. So from Eqs. (B49), (B51), (B53) the upper limit M_1 and lower limit M_2 of u can be obtained:

$$M_1 = \min(B_0, B_+), \quad M_2 = \max(k_{\tau_\alpha}, B_-). \tag{B55}$$

From Eq. (B35) it can be obtained that

$$-2k_\alpha t \leqslant z \leqslant 2k_\alpha t. \tag{B56}$$

According to Eq. (B41) the variable z satisfies

$$z \geqslant k_\alpha^2 + t^2 - 4s_h^2. \tag{B57}$$

From Eqs. (B56) and (B57) it can be obtained that the upper limit of z is $2k_\alpha t$, the lower limit of z is

$$Z = \begin{cases} k_\alpha^2 + t^2 - 4s_h^2 & t > 2s_h - k_\alpha \\ -2k_\alpha t & t \leqslant 2s_h - k_\alpha \end{cases}. \tag{B58}$$

From Eqs. (B56) and (B57) it can be also obtained that

$$t^2 - 2k_\alpha t + k_\alpha^2 - 4s_h^2 \leqslant 0. \tag{B59}$$

Thus the upper limit T_1 and lower limit T_2 of t can be obtained

$$T_1 = k_\alpha + 2s_h, \tag{B60}$$

$$T_2 = \begin{cases} k_\alpha - 2s_h & 2s_h < k_\alpha \\ 0 & 2s_h \geqslant k_\alpha \end{cases}. \tag{B61}$$

From Eqs. (B49) and (B51) it can be obtained that

$$k_{\tau_\alpha}^2 \leqslant k_\alpha^2 - \frac{2\beta_{\tau_v}}{\beta_{\tau_\alpha}}\left(k_{\tau_v}^2 - s_h^2\right). \tag{B62}$$

Thus the lower limit of s_h can be obtained

$$H = \begin{cases} \left[k_{\tau_v}^2 - \frac{\beta_{\tau_\alpha}}{2\beta_{\tau_v}}\left(k_\alpha^2 - k_{\tau_\alpha}^2\right)\right]^{1/2} & k_\alpha^2 < k_{\tau_\alpha}^2 + \frac{2\beta_{\tau_v}}{\beta_{\tau_\alpha}}k_{\tau_v}^2 \\ 0 & k_\alpha^2 \geqslant k_{\tau_\alpha}^2 + \frac{2\beta_{\tau_v}}{\beta_{\tau_\alpha}}k_{\tau_v}^2 \end{cases}. \tag{B63}$$

Finally Eq. (B38) can be written as

$$I_B(\tau_\alpha, \tau_v, \tau_v) = \frac{4\pi^4}{\beta_{\tau_v}k_\alpha}\int_H^{k_{\tau_v}} s_h \mathrm{d}s_h \int_{T_2}^{T_1} \mathrm{d}t \int_Z^{2k_\alpha t} f_1 \mathrm{d}z \times \int_{M_2}^{M_1} u\mathrm{d}u \int_{-2tu}^{N} f_2 \mathrm{d}w. \tag{B64}$$

In the case of $\tau_\zeta \neq \tau_v$, the δ function in the integral $I_B(\tau_\alpha, \tau_v, \tau_\zeta)$ given by Eq. (B10) is dependent on $\cos\alpha_p$ and $\cos\alpha_h$ and independent on φ_p and φ_h. We have

$$\int \mathrm{d}\vec{q}_p = 2\pi \int q_p^2 \mathrm{d}q_p \int \mathrm{d}\cos\alpha_p, \qquad \int \mathrm{d}\vec{q}_h = 2\pi \int q_h^2 \mathrm{d}q_h \int \mathrm{d}\cos\alpha_h. \tag{B65}$$

With the similar way the reduced formula of the integral $I_B(\tau_\alpha, \tau_v, \tau_\zeta)$ in the case of $\tau_\zeta \neq \tau_v$ can be obtained as follows:

$$I_B(\tau_\alpha, \tau_v, \tau_\zeta) = \frac{4\pi^4}{\beta_- k_\alpha}\int_{H_2}^{H_1} s_h \mathrm{d}s_h \int_{T_2}^{T_1} \mathrm{d}t \times \int_Z^{2k_\alpha t} q_h \mathrm{d}z \int_{D_2}^{D_1} \mathrm{d}\cos\alpha_h \int_{P_2}^{P_1} s_p \mathrm{d}s_p \times \int_{M_2}^{M_1} u\mathrm{d}u \int_{-2tu}^{N} \frac{\mathrm{d}w}{k_p}\Theta(A_1 - S)\Theta(S - A_2), \tag{B66}$$

where

$$S = \frac{1}{\beta_- k_p q_p}\left(\beta_{\tau_\alpha}k_\alpha^2 + \beta_+ s_h^2 + \beta_- k_h q_h \cos\alpha_h - \beta_+ s_p^2 - \beta_{\tau_\alpha}u^2\right), \tag{B67}$$

$$A_1 = \min(1, A_{\tau_\zeta}), \quad A_2 = \max(-1, -A_{\tau_v}), \tag{B68}$$

$$A_{\tau_v} = \frac{\frac{1}{4}k_p^2 + q_p^2 - k_{\tau_v}^2}{k_p q_p}, \quad A_{\tau_\zeta} = \frac{\frac{1}{4}k_p^2 + q_p^2 - k_{\tau_\zeta}^2}{k_p q_p}, \tag{B69}$$

$$N = \begin{cases} 4s_p^2 - t^2 - u^2 & u > 2s_p - t \\ 2tu & u \leqslant 2s_p - t \end{cases}, \tag{B70}$$

$$M_1 = B_+, \quad M_2 = \max(k_{\tau_\alpha}, B_-), \quad B_\pm = t \pm 2s_p, \tag{B71}$$

$$P_1^2 = \frac{1}{2}\left(k_{\mu,\max}^2 + k_{\xi,\max}^2\right) \tag{B72}$$

$$P_2 = \begin{cases} \left\{\frac{1}{\beta_+}\left[\beta_{\tau_v}k_{\tau_v}^2 + \beta_{\tau_\zeta}k_{\tau_\zeta}^2 - \frac{1}{2}\beta_-\left(k_{\mu,\max}^2 + k_{\xi,\max}^2\right)\right]\right\}^{1/2} \\ \quad \text{for } \beta_{\tau_v}k_{\tau_v}^2 + \beta_{\tau_\zeta}k_{\tau_\zeta}^2 > \frac{1}{2}\beta_-\left(k_{\mu,\max}^2 + k_{\xi,\max}^2\right), \\ 0 \quad \text{for } \beta_{\tau_v}k_{\tau_v}^2 + \beta_{\tau_\zeta}k_{\tau_\zeta}^2 \leqslant \frac{1}{2}\beta_-\left(k_{\mu,\max}^2 + k_{\xi,\max}^2\right) \end{cases} \tag{B73}$$

$$k_{\mu,\max}^2 = \frac{1}{\beta_{\tau_v}}\left[\beta_{\tau_\alpha}\left(k_\alpha^2 - k_{\tau_\alpha}^2\right) + \beta_{\tau_v}k_{\tau_v}^2\right], \qquad k_{\xi,\max}^2 = \frac{1}{\beta_{\tau_\zeta}}\left[\beta_{\tau_\alpha}\left(k_\alpha^2 - k_{\tau_\alpha}^2\right) + \beta_{\tau_\zeta}k_{\tau_\zeta}^2\right], \tag{B74}$$

$$D_1 = \min(1, D_{\tau_v}), \quad D_2 = \max(-1, -D_{\tau_\zeta}), \tag{B75}$$

$$D_{\tau_v} = \frac{k_{\tau_v}^2 - \frac{1}{4}k_h^2 - q_h^2}{k_h q_h}, \quad D_{\tau_\zeta} = \frac{k_{\tau_\zeta}^2 - \frac{1}{4}k_h^2 - q_h^2}{k_h q_h}, \tag{B76}$$

$$H_1^2 = \frac{1}{2}\left(k_{\tau_v}^2 + k_{\tau_\zeta}^2\right), \tag{B77}$$

$$H_2 = \begin{cases} \left\{\frac{1}{\beta_+}\left[\beta_{\tau_v}k_{\tau_v}^2 + \beta_{\tau_\zeta}k_{\tau_\zeta}^2 - \beta_{\tau_\alpha}\left(k_\alpha^2 - k_{\tau_\alpha}^2\right) - \frac{1}{2}\beta_-\left(k_{\tau_v}^2 + k_{\tau_\zeta}^2\right)\right]\right\}^{1/2} \\ \qquad \text{for } \beta_{\tau_v}k_{\tau_v}^2 + \beta_{\tau_\zeta}k_{\tau_\zeta}^2 > \beta_{\tau_\alpha}\left(k_\alpha^2 - k_{\tau_\alpha}^2\right) + \frac{1}{2}\beta_-\left(k_{\tau_v}^2 + k_{\tau_\zeta}^2\right) \\ 0 \qquad \text{for } \beta_{\tau_v}k_{\tau_v}^2 + \beta_{\tau_\zeta}k_{\tau_\zeta}^2 \leqslant \beta_{\tau_\alpha}\left(k_\alpha^2 - k_{\tau_\alpha}^2\right) + \frac{1}{2}\beta_-\left(k_{\tau_v}^2 + k_{\tau_\zeta}^2\right) \end{cases}. \tag{B78}$$

The variables $\beta_+, \beta_-, k_h, q_h, k_p, q_p, Z, T_1, T_2$ in Eq. (B66) are given in Eqs. (B9), (B40)–(B43), (B58), (B60), (B61), respectively. $\Theta(x)$ is the step function given by Eq. (A28).

[1] J. S. Bell and E. J. Squires, Phys. Rev. Lett. **3**, 96 (1959); J. S. Bell, in *Lectures on the Many-Body Problem*, edited by E. R. Caianiello (Academic Press, New York, 1962), p. 91.
[2] M. K. Weigel, *Microscopic Optical Potentials*, *Lecture Notes in Physics*, Vol. 89 (Springer Berlin, Heidelberg, New York, 1979), p. 56.
[3] J. P. Jeukenne, A. Lejeune, and C. Mahaux, Phys. Rep. **25**, 83 (1976).
[4] J. P. Jeukenne, A. Lejeune, and C. Mahaux, Phys. Rev. C **16**, 80 (1977).
[5] F. A. Brieva and J. R. Rook, Nucl. Phys. **A291**, 317 (1977).
[6] N. Vinh Mau and A. Bouyssy, Nucl. Phys. **A257**, 189 (1976).
[7] V. Bernard and Nguyen Van Giai, Nucl. Phys. **A327**, 397 (1979); **A348**, 75 (1980).
[8] Q. B. Shen, J. S. Zhang, and Y. Z. Zhuo, Nucl. Phys. **3**, 232 (1981) (in Chinese).
[9] Q. B. Shen, J. S. Zhang, Y. Tian, Z. Y. Ma, and Y. Z. Zhuo, Z. Phys. A **303**, 69 (1981).
[10] Q. B. Shen, J. S. Zhang, Y. Tian, and Y. Z. Zhuo, High Energy Phys. Nucl. Phys. **6**, 91 (1982) (in Chinese).
[11] Q. B. Shen, Y. Tian, Z. Y. Ma, J. S. Zhang, and Y. Z. Zhuo, High Energy Phys. Nucl. Phys. **6**, 185 (1982) (in Chinese).
[12] Q. B. Shen, Y. Tian, J. S. Zhang, and Y. Z. Zhuo, *Nuclear Data for Science and Technology, Proceedings of the International Conference, 6–10 September 1982* (Antwerp, Belgium, 1983), p. 565.
[13] Q. B. Shen, Y. Tian, J. S. Zhang, and Y. Z. Zhuo, Commun. Theor. Phys. **2**, 1233 (1983).
[14] C. H. Cai, Q. B. Shen, and Y. Z. Zhuo, Nucl. Sci. Eng. **109**, 142 (1991).
[15] D. Vautherin and D. M. Brink, Phys. Rev. C **5**, 626 (1972).
[16] J. W. Negele and D. Vautherin, Phys. Rev. C **5**, 1472 (1972).
[17] S. Krewald, V. Klemt, J. Speth, and A. Faessler, Nucl. Phys. **A281**, 166 (1977).
[18] H. Orland and R. Schaeffer, Nucl. Phys. **A299**, 442 (1978).
[19] R. Sartor and C. Mahaux, Phys. Rev. C **21**, 1546 (1980).
[20] V. Bernard and C. Mahaux, Phys. Rev. C **23**, 888 (1981).
[21] Q. B. Shen, Z. X. Li, X. J. Shi, Y. Tian, and Y. Z. Zhuo, in *Proceedings of the International Summer School on Nucleon-Nucleon Interaction and Nuclear Many-Body Problem, July 1983* (Changchun, China, 1984), p. 618.
[22] Q. B. Shen, Z. X. Li, X. J. Shi, Y. Tian, and Y. Z. Zhuo, High Energy Phys. Nucl. Phys. **9**, 220 (1985) (in Chinese); Chin. Phys., **5**, 925 (1985).
[23] Q. B. Shen, Y. Tian, Z. X. Li, and Y. Z. Zhuo, High Energy Phys. Nucl. Phys. **9**, 327 (1985) (in Chinese).
[24] L. X. Ge, Y. Z. Zhuo, and W. Norenberg, Nucl. Phys. **A459**, 77 (1986).
[25] Y. L. Han, X. Z. Wu, and Y. Z. Zhuo, High Energy Phys. Nucl. Phys. **12**, 257 (1988) (in Chinese).
[26] Y. Z. Zhuo, Y. L. Han, and X. Z. Wu, Prog. Theor. Phys. **79**, 110 (1988).
[27] M. Beiner, H. Flocard, Nguyen Van Giai, and P. Quentin, Nucl. Phys. **A238**, 29 (1975).
[28] J. Treiner and H. Krivine, J. Phys. G **2**, 285 (1976).
[29] H. S. Kohler, Nucl. Phys. **A258**, 301 (1976).
[30] H. Krivine, J. Treiner, and O. Bohigas, Nucl. Phys. **A336**, 155 (1980).
[31] Nguyen Van Giai and H. Sagawa, Phys. Lett. **B106**, 379 (1981).
[32] L. Bennour, P. H. Heenen, P. Bonche, J. Dobaczewski, and H. Flocard, Phys. Rev. C **40**, 2834 (1989).
[33] J. W. Negele, Phys. Rev. C **1**, 1260 (1970).
[34] Q. B. Shen, Y. Tian, and R. Z. Liu, High Energy Phys. Nucl. Phys. **7**, 473 (1983) (in Chinese).
[35] F. D. Becchetti and G. W. Greenlees, Phys. Rev. **182**, 1190 (1969).
[36] R. W. Finlay, W. P. Abfalterer, G. Fink *et al.*, Phys. Rev. C **47**, 237 (1993).
[37] D. C. Larson, J. A. Harvey, and N. W. Hill, *Symposium on Neutron Cross Sections at 10–50 MeV* (Brookhaven, 1980), p. 277.
[38] J. R. Morales, L. O. Figueroa, J. L. Romero *et al.*, Nucl. Instrum. Methods Phys. Res. A **300**, 312 (1991).
[39] M. H. Macgregor, W. P. Ball, and R. Booth, Phys. Rev. **108**, 726 (1957).
[40] M. H. Macgregor, W. P. Ball, and R. Booth, Phys. Rev. **111**, 1155 (1958).
[41] W. P. Ball, M. H. Macgregor, and R. Booth, Phys. Rev. **110**, 1392 (1958).
[42] B. Pal, A. Chatterjee, and A. M. Ghose, Nucl. Instrum. Methods Phys. Res. **171**, 347 (1980).
[43] A. Chatterjee and A. M. Ghose, Phys. Rev. **161**, 1181 (1967).

[44] V. I. Strizhak, At. Ener. **2**, 68 (1957).
[45] J. G. Degtjarev and V. G. Nadtochij, At. Ener. **11**, 397 (1961).
[46] I. A. Korzh and V. A. Mishchenko *et al.*, Ukr. Fiz. Zh. **13**, 1781 (1968).
[47] D. J. Bredin, Phys. Rev. **135**, 412 (1964).
[48] T. Schweitzer, D. Seeliger, and S. Unholzer (private communication, 1978).
[49] X. Wang, Y. Wang, D. Wang, and J. Rapaport, Nucl. Phys. **A465**, 483 (1987).
[50] G. Dagge, W. Grum, J. W. Hammer, K. W. Hoffmann, and G. Schreder, Phys. Rev. C **39**, 1768 (1989).
[51] J. D. Brandenberger, A. Mittler, and M. T. McEllistrem, Nucl. Phys. **A196**, 65 (1972).
[52] D. E. Velkley, D. W. Glasgow *et al.*, Phys. Rev. C **9**, 2181 (1974).
[53] C. S. Whisnant, J. H. Dave, and C. R. Gould, Phys. Rev. C **30**, 1435 (1984).
[54] L. F. Hansen, F. S. Dietrich, B. A. Pohl, C. H. Poppe, and C. Wong, Phys. Rev. C **31**, 111 (1985).
[55] M. M. Nagadi, C. R. Howell *et al.*, Phys. Rev. C **68**, 044610 (2003).
[56] J. S. Petler, M. S. Islam, R. W. Finlay, and F. S. Dietrich, Phys. Rev. C **32**, 673 (1985).
[57] G. L. Salmon, Nucl. Phys. **21**, 15 (1960).
[58] K. Bearpark, W. R. Graham, and G. Jones, Nucl. Phys. **73**, 206 (1965).
[59] N. Okumura, Y. Aoki, T. Joh, Y. Honkyu, K. Hirota, and K. S. Itoh, Nucl. Instrum. Methods Phys. Res. A **487**, 565 (2002).
[60] R. E. Pollock and G. Schrank, Phys. Rev. **140**, 575 (1965).
[61] M. Q. Makino, C. N. Waddell, and R. M. Eisberg, Nucl. Phys. **50**, 145 (1964).
[62] B. D. Wilkins and G. Igo, Phys. Rev. **129**, 2198 (1963).
[63] P. Kirkby and W. T. Link, Can. J. Phys. **44**, 1847 (1966).
[64] M. Chiari, L. Giuntini, P. A. Mando, and N. Taccetti, Nucl. Instrum. Methods Phys. Res. B **174**, 259 (2001).
[65] R. Roy, C. R. Lamontagne *et al.*, Nucl. Phys. **A411**, 1 (1983).
[66] G. M. Crawley, Ph.D. thesis (1965).
[67] R. Dittman, H. S. Sandhu, R. K. Cole, and C. N. Waddell, Nucl. Phys. **A126**, 592 (1969).
[68] C. B. Fulmer, J. B. Ball, A. Scott, and M. L. Whiten, Phys. Rev. **181**, 1565 (1969).
[69] F. E. Bertrand and R. W. Peelle, Phys. Rev. C **8**, 1045 (1973).
[70] G. Gerstein, J. Niederer, and K. Strauch, Phys. Rev. **108**, 427 (1957).
[71] J. A. Harvey (private communication, 1987).
[72] E. Cornelis, L. Mewissen, and F. Poortmans, *Conference on Nuclear Data for Science and Technology, 6–10 September 1982* (Antwerp, Belgium, 1983), p. 135.
[73] W. P. Abfalterer, F. B. Bateman, F. S. Dietrich, R. W. Finlay, R. C. Haight, G. L. Morgan, Phys. Rev. C **63**, 044608 (2001).
[74] J. G. Degtjarev, At. Ener. **19**, 456 (1965).
[75] C. Zanelli, P. Urone *et al.*, Phys. Rev. C **23**, 1015 (1981).
[76] A. I. Abramov, At. Ener. **12**, 62 (1962).
[77] N. Olsson, B. Trostell, E. Ramstroem, and B. Holmqvist, Nucl. Phys. **A472**, 237 (1987).
[78] T. P. Stuart, J. D. Anderson, and C. Wong, Phys. Rev. **125**, 276 (1962).
[79] S. Mellema, R. W. Finlay, F. S. Dietrich, and F. Petrovich, Phys. Rev. C **28**, 2267 (1983).
[80] J. F. Dicello, G. J. Igo, and M. L. Roush, Phys. Rev. **157**, 1001 (1967).
[81] R. H. Mccamis, N. E. Davison *et al.*, Can. J. Phys. **64**, 685 (1986).
[82] J. J. Menet, E. E. Gross, J. J. Malanify, and A. Zucker, Phys. Rev. Lett. **22**, 1128 (1969).
[83] N. Boukharouba, C. E. Brient, S. M. Grimes, V. Mishra, and R. S. Pedroni, Phys. Rev. C **46**, 2375 (1992).
[84] J. Benveniste, A. C. Mitchell, B. Buck, and C. B. Fulmer, Phys. Rev. **133**, 323 (1964).
[85] R. Varner, Phys. Rep. **201**, 57 (1991).
[86] P. Kossanyi-Demay, R. De Swiniarski, and C. Glashausser, Nucl. Phys. **A94**, 513 (1967).
[87] S. F. Eccles, H. F. Lutz, and V. A. Madsen, Phys. Rev. **141**, 1067 (1966).
[88] B. W. Ridley and J. F. Turner, Nucl. Phys. **58**, 497 (1964).
[89] M. K. Brussel and J. H. Williams, Phys. Rev. **114**, 525 (1959).
[90] R. De Leo, H. Akimune *et al.*, Phys. Rev. C **53**, 2718 (1996).
[91] J. A. Harvey (private communication, 1999).
[92] G. M. Haas and P. L. Okhuysen, Phys. Rev. **132**, 1211 (1963).
[93] G. Haouat, J. Sigaud, J. Lachkar, C. Lagrange, B. Duchemin, and Y. Patin, Nucl. Sci. Eng. **81**, 491 (1982).
[94] J. R. M. Annand, R. W. Finlay, and F. S. Dietrich, Nucl. Phys. **A443**, 249 (1985).
[95] M. L. Roberts, P. D. Felsher *et al.*, Phys. Rev. C **44**, 2006 (1991).
[96] J. Rapaport, T. S. Cheema, D. E. Bainum, R. W. Finlay, and J. D. Carlson, Nucl. Phys. **A296**, 95 (1978).
[97] J. P. Delaroche, C. E. Floyd, P. P. Guss, R. C. Byrd, K. Murphy, G. Tungate, and R. L. Walter, Phys. Rev. C **28**, 1410 (1983).
[98] C. E. Floyd, Ph.D. thesis (1981).
[99] J. H. Osborne, F. P. Brady *et al.*, Phys. Rev. C **70**, 054613 (2004).
[100] A. Ingemarsson, J. Nyberg *et al.*, Nucl. Phys. **A653**, 341 (1999).
[101] A. Auce and A. Ingemarsson *et al.*, Phys. Rev. C **71**, 064606 (2005).
[102] J. J. Menet, E. E. Gross, J. J. Malanify, and A. Zucker, Phys. Rev. C **4**, 1114 (1971).
[103] J. F. Turner, B. W. Ridley, P. E. Cavanagh, G. A. Gard, and A. G. Hardacre, Nucl. Phys. **58**, 509 (1964).
[104] R. F. Carlson, A. J. Cox *et al.*, Phys. Rev. C **12**, 1167 (1975).
[105] W. T. H. Van Oers, H. Haw, N. E. Davison, A. Ingemarsson, B. Fagerstroem, and G. Tibell, Phys. Rev. C **10**, 307 (1974).
[106] L. N. Blumberg, E. E. Gross, A. Van der Woude, A. Zucker, and R. H. Bassel, Phys. Rev. **147**, 812 (1966).
[107] A. Nadasen, P. Schwandt *et al.*, Phys. Rev. C **23**, 1023 (1981).